

**LAYER SPECIFIC DISTRIBUTION OF MUSCARINIC  
RECEPTOR M2 IN THE SENSORIMOTOR AREAS OF RAT  
BRAIN**

by

**Sedef YUSUFOĞULLARI**

B.Sc., in Biology, Çukurova University, 2010

Submitted to the Institute of Biomedical Engineering  
in partial fulfillment of the requirements  
for the degree of  
Master of Science  
in  
Biomedical Engineering

Boğaziçi University

2018

## ACKNOWLEDGMENTS

I would like to take this opportunity to thank all my colleagues who helped and supported me throughout this project. My special gratitude goes to my thesis supervisor Prof. Dr. Burak Güçlü, who gave me the opportunity to conduct this study, as well as his great help and guidance throughout the experimental work and writing process. His feedback and advice were invaluable. I also wish to express my profound gratitude to the Bige Vardar for providing me with constant help. I'd like to express my special thanks to Deniz Kılınç for the assistance during the experiment. Furthermore I would like to thank to Çağlar Gök, Elçin Tunçkol, İsmail Devecioğlu, İpek Toker Karakuş, Rima Çelik, and Shervin Bashiri. Finally, I'm grateful to my family for their helping throughout entire process. I would be grateful forever for their support.

## ACADEMIC ETHICS AND INTEGRITY STATEMENT

I, Sedef YUSUFOĞULLARI, hereby certify that I am aware of the Academic Ethics and Integrity Policy issued by the Council of Higher Education (YÖK) and I fully acknowledge all the consequences due to its violation by plagiarism or any other way.

Name :

---

Signature:

---

Date:

---

## ABSTRACT

### LAYER SPECIFIC DISTRIBUTION OF MUSCARINIC RECEPTOR M2 IN THE SENSORIMOTOR AREAS OF RAT BRAIN

Current understanding of attentional mechanisms within the tactile modality is not fully known. We have recently studied muscarinic receptor-mediated responses of vibrotactile neurons which vary according to cortical depth due to the differences in the local connectivity in the cortex. The aim of this study is to characterize specific muscarinic receptor subtype (M2) by immunofluorescence technique for understanding the role of these receptors within the associated cortex. In particular, differences between barrel field (S1BF), motor cortex (M1) and hindlimb area (S1HL) of the rat SI were investigated. Coronal sections ( $50 \mu m$ ) from 7 Wistar Albino rats were obtained for each area. Mouse monoclonal anti-mAChR2 was used as primary antibody and goat anti-IgG1 with Alexa Fluor 594 was used as secondary antibody. Ethidium bromide was used on additional sections to determine layer thicknesses and total number of cells within a layer. Statistical analyses were performed on three dependent variables: Average number of M2 receptor complexes (M2RC) in a layer (N), average number of M2RC normalized with layer thickness (D), and average number of M2RC per total number of cells in a layer (C). 2-way ANOVA showed significant main effects of layer on N, D, and C ( $p < 0.001$ ,  $p = 0.002$ ,  $p = 0.053$ , respectively). Area and layer interaction was only observed for N ( $p < 0.001$ ). On the other hand, area did not have a main effect for any dependent variable. The number of M2RC was highest in layer V, VI, IV for M1, S1BF and S1HL, respectively. Additionally, when the average number M2RC were normalized according to thickness, highest M2 density were observed in layer II and III for all areas. In other layers, M2 density was similar for S1HL and S1BF, but lower than M1. There was no general difference among the three cortical area regarding the number and density of M2RC which is consistent with the cholinergic innervation in the sensory-motor areas. However, the distribution of M2RC varied within each area. **Keywords:** Somatosensory, Cortex, Immunofluorescence, Cholinergic, Attention.

## ÖZET

### SIÇAN BEYNİNDEKİ DUYU-MOTOR ALANLARINDA MUSKARİNİK RESEPTÖR M2 KOMPLEKSİN KATMANSAL DAĞILIMI

Dokunmayla ilişkili nöron aktivitesinin dikkate bağlıdeğişimi tam olarak bilinmemektedir. Önceki çalışmamızda kolinerjik reseptörlerin birincil beden duyusu korteksindeki titreşimsel uyarılabilen nöronlar üzerindeki etkilerini inceledik ve muskarinik reseptör bağlantılıyanıtların korteks katmanlarına göre değiştiğini gördük. Temel sebep kortekste lokal bağlantısal farklılıklardır. Tez çalışmamızın amacı kortekste bulunan muskarinik reseptör 2 (M2)'yi immünfloresans tekniği ile işaretlemektir. Böylece M2'nin dağılımı daha iyi görülebilecek ve devre yapısında anlaşılacaktır. Ayrıca, motor korteks ve birincil beden duyusu korteksi bıyık alanı ve arka ayak alanı arasındaki farklar incelenebilir. Yedi Wistar albino sıçanda ilgili beyin alanlarından 50  $\mu m$  kalınlığında koronal kesitler alınmıştır. Primer antikor olarak fare monoclonal anti-mAChR2 (IgG1) antikor ve sekonder antikor olarak da Alexa Fluor 594 kullanılmıştır. Katman kalınlığı ve toplam hücre sayısını için bazı kesitler etidyum bromit ile boyanmış. M2 reseptör kompleksi (M2RK) manuel olarak sayılmış ve istatistiksel analizler üç farklı bağımlı değişken üzerinden yapılmıştır: katmandaki ortalama M2 reseptör kompleks sayısı (N), katman kalınlığına göre normalize edilmiş ortalama M2 reseptör kompleks yoğunluğu (D) ve katmandaki ortalama M2 reseptör kompleks sayısının toplam hücre sayısına oranı (C). İki Yönlü ANOVA sonuçlarına göre N, D ve C için katman ana etki olarak çıkmıştır (sırasıyla  $p<0.001$ ,  $p=0.002$ ,  $p=0.053$ ). Sadece N için korteks alanı ve katman arasında anlamlı bir etkileşim olmuştur ( $p<0.001$ ). Ancak hiç bir değişken için korteks alanlar ana etki olarak çıkmamıştır. En fazla M2RK sayısı sırasıyla M1, S1BF ve S1HL için katman V, VI ve IV'tür. Ayrıca, ortalama M2RK sayısı katman kalınlığına göre normalize edildiğinde, M2RK yoğunluğu tüm alanlar için katman II ve III'te bulunmuştur. M2 yoğunluğu diğer katmanlarda S1HL ve S1BF için benzer ancak M1'den azdır. Sonuçlar beyindeki genel kolinerjik inervasyonla uyumlu olup, üç alan arasında bir farklılık vardır. Fakat, her alan içinde M2RK farklılık göstermektedir.

## TABLE OF CONTENTS

ACKNOWLEDGMENTS . . . . .	iii
ACADEMIC ETHICS AND INTEGRITY STATEMENT . . . . .	iv
ABSTRACT . . . . .	v
ÖZET . . . . .	vi
LIST OF FIGURES . . . . .	ix
LIST OF TABLES . . . . .	xi
LIST OF ABBREVIATIONS . . . . .	xii
1. INTRODUCTION . . . . .	1
1.1 Outline . . . . .	2
2. BACKGROUND . . . . .	3
2.1 Attention and Cholinergic System . . . . .	3
2.2 Cholinergic receptors . . . . .	6
2.2.1 Nicotinic Receptors . . . . .	6
2.2.2 Muscarinic Receptors . . . . .	7
2.3 Cytoarchitecture of the Neocortex . . . . .	10
2.4 Localization of Cholinergic Receptors in the Cortex . . . . .	12
2.5 Aim of the Study . . . . .	13
3. MATERIALS AND METHODS . . . . .	15
3.1 Animals . . . . .	15
3.2 Fixation and Brain sectioning . . . . .	15
3.3 Nissl Staining . . . . .	16
3.4 Immunostaining . . . . .	16
3.5 Counterstaining for Immunofluorescence . . . . .	17
3.6 Antibody staining . . . . .	19
3.7 Cell Counting . . . . .	21
3.8 Statistical Analysis . . . . .	23
3.8.1 Nissl stained data . . . . .	23
3.8.2 Immunostained data . . . . .	23
4. RESULTS . . . . .	24

4.1	Nissl Staining . . . . .	24
4.2	Muscarinic receptor M2 staining . . . . .	26
5.	DISCUSSION and CONCLUSION . . . . .	36
5.1	Comparison of Nissl staining with literature and future work . . . . .	36
5.2	Comparison of immunostaining with previous literature . . . . .	37
5.3	Future work . . . . .	38
6.	Appendix A . . . . .	39
7.	Appendix B . . . . .	42
	REFERENCES . . . . .	45

## LIST OF FIGURES

Figure 2.1	Working system of the ACh in the synaptic cleft (Adopted from [17]).	4
Figure 2.2	Schematic diagram of posterior and anterior attention system and their elements [5].	5
Figure 2.3	Structure of nAChRs [40].	7
Figure 2.4	Structure of mAChRs (Adopted from [69]).	9
Figure 2.5	Detailed columnar structure of Neocortex [71].	10
Figure 2.6	Neural circuits in the cortex (G: granule cell, H: horizontal cell, M: Martinotti cell, P: pyramidal cell, S: stellate cell. The arrows in the figure shows the information flow)[73].	12
Figure 3.1	Flow diagram of Nissl Staining.	17
Figure 3.2	Pictures with different magnifications (X100 and X400).	18
Figure 3.3	Excitation and emission spectra for Ethidium Bromide (EtBr) [76].	19
Figure 3.4	A sample of EtBr (rat 218 sld7- s1bf 2).	20
Figure 3.5	Excitation and emission values of Alexa Flour 594 [77].	21
Figure 3.6	Schematic showing the hemispheric width boundaries as well as the midline distance measurements in for each area.	22
Figure 4.1	Nissl staining for measuring the length of M1 in Neocortex.	24
Figure 4.2	Nissl staining for measuring the length of S1HL in Neocortex.	25
Figure 4.3	Nissl staining for measuring the length of S1BF in Neocortex.	26
Figure 4.4	Total thickness of the layers in relevant areas (M1, S1HLand S1BF) (Error bars are indicated in SEM).	28
Figure 4.5	The thickness of layers in M1, S1-hind leg and Barrel cortex (Error bars are indicated in SEM, p-values denotes **<0.05, * * *<0.005)).	28
Figure 4.6	EtBr staining for quantifying the total number of cells in M1. Horizontal green lines indicate layer boundaries. Green small dots indicate counted cells (Rat 217-slide 1-Magnification x20).	30

Figure 4.7	EtBr staining for quantifying the total number of cells in S1HL. Horizontal green lines indicates layer boundaries. Green small dots indicates counted samples (Rat 216-slide 7-Magnification x20).	30
Figure 4.8	EtBr staining for quantifying the total number of cells in S1HL. Horizontal green lines indicated layer boundaries. Green small dots indicates counted samples (Rat 217-slide 1-Magnification x20).	31
Figure 4.9	M2 immunostaining in S1BF. (Rat 219-slide 2-Magnification x20).	31
Figure 4.10	M2 immunostaining in M1. (Rat 222-slide 2-Magnification x20).	32
Figure 4.11	Distribution of average number of M2RC (N) through all layers for each are. All bars are shown as Mean + SEM.	32
Figure 4.12	Distribution of average number of M2RC per mm layer thickness (D) through all layers for each area. All bars are shown as Mean + SEM.	33
Figure 4.13	Distribution of average number of M2RC per total number of cells(C) through all layers for each area. All bars are shown as Mean + SEM.	33
Figure 4.14	Distribution of average number of M2RC (N) through all layers by sex for each area. All bars are shown as Mean + SEM.	34
Figure 4.15	Distribution of average number of M2RC per mm layer thickness (D) through all layers by sex for each area. All bars are shown as Mean + SEM.	34
Figure 4.16	Distribution of average number of M2RC per total number of cells(C) through all layers by sex for each area. All bars are shown as Mean + SEM.	35

## LIST OF TABLES

Table 4.1	The average layer thicknesses measured from different cortical areas.	27
Table 4.2	Average number of M2RC (N), average number of M2RC per mm thickness (D) and average number of M2RC per total number of cells (C) for each area (M1, S1HL, and S1BF).	29

## LIST OF ABBREVIATIONS

acetyl CoA	Acetyl Coenzyme A
ACh	Acetylcholine
AChE	Acetylcholinesterase
AD	Alzheimer disease
ADD	Attention Deficit Disorder
ChAT	Choline Acetyltransferase
CNS	Central Nervous System
EtBr	Ethidium Bromide
IHC	Immunohistochemistry
IP	Intraperitoneally
M1	Primary Motor Cortex
M2	Muscarinic receptor type 2
mAChRs	Muscarinic receptors
nAChRs	Nicotinic receptors
NBF	Neutral Buffered Formalin
NGS	Normal Goat serum
PBS	Phosphate Buffered Saline
PBTx	PB with Triton X-100
PBTxg	Goat serum
PFA	Neutral Buffered Paraformaldehyde
PFC	Prefrontal cortex
PNS	Peripheral Nervous System
S1BF	Barrel field
S1HL	Hindpaw representation of SI cortex
SI	Primary Somatosensory Cortex

## 1. INTRODUCTION

Attention is a complex behavioral and cognitive process of allocating cognitive processing resources to focus on someone or something interesting while ignoring others. We orient either by the movement of eyes and head (overt shift of attention) or without shifting of the head and eyes (covert shift of attention) [1, 2]. It is considered that this cognitive shift involves the cholinergic system and it is accompanied by increased acetylcholine (ACh) levels in the brain. This system is necessary for cognitive functions that depend on attention [3–6]. According to findings by Sarter et. al [5], cholinergic system has an effect on attentional processes via two mechanisms; bottom-up and top-down. According to the bottom-up mechanism, sensory inputs from the external world often drive our attention based on characteristics of stimuli. In top-down modulation mechanism, the brain is capable of directing attention toward or away from the stimuli based on our previous experiences. Whatever the mechanism is, attention depends on the cholinergic system which is mediated by nicotinic (nAChRs) and muscarinic (mAChRs) receptors. Basal forebrain is one of the main centers of the brain including cholinergic neurons. These neurons and their axons from the specific nucleus of the basal forebrain (nucleus basalis of Meynert) to the cortex. Studies have shown that decline in the number of the cholinergic neurons in the basal forebrain is the main reason of decreasing cholinergic input to the cortex. Thus, it may be one reason for some deficits in Alzheimer’s disease (AD) [7]. Immunochemical labeling techniques helped us to determine mAChRs and nAChRs in the rat frontal/motor and parietal cortex at the neural and sub neural level [8], [9–12]. However, little attention was given to the detailed distribution of cholinergic receptors in neocortex specifically in the sensory and motor areas, which are essential part of understanding the mechanism of cholinergic system related with disease such as AD and attention deficit disorder (ADD). Therefore, the physiological and morphological characterization of cholinergic receptors in the sensorimotor areas of the rat cortex would contribute to the understanding of attentional modulation of tactile input. In this master thesis, the distribution of muscarinic receptor type 2 (M2) will be investigated in three areas of the rat neocortex; barrel

field (S1BF), hindpaw representation of SI cortex (S1HL), and primary motor cortex (M1). The results will be useful for ongoing research about a computational model of vibrotactile neurons in the rat cortex.

## 1.1 Outline

The thesis consists of four chapters. The first Chapter presents the background information about the relationship between attention and cholinergic system, the cytoarchitecture of the brain (layers and neuron types) and the cholinergic receptors found in the brain. In Chapter 2, the methods and materials used in the experiments are explained. In Chapter 3, the results of performed experiments and statistical computations are presented. The fourth Chapter presents conclusion and discussion about results and the recommended future work.

## 2. BACKGROUND

### 2.1 Attention and Cholinergic System

Acetylcholine (ACh) is the first identified and the most common neurotransmitter in the body. In general, it is an excitatory neurotransmitter. Biosynthesis of the chemical is made by choline acetyltransferase (ChAT). The enzyme assembles Acetyl coenzyme A (acetyl CoA), which is glucose-derived molecule, and choline. With the high hydrolysis capability of acetylcholinesterase (AChE) the action of ACh is terminated. ACh can be found in all parts of the nervous system. In the peripheral nervous system (PNS) it is located either in muscle tissues to control the neuromuscular mechanisms, and synapses in the autonomic nervous system to regulate the viscera. In the central nervous system, it is located in many places such as the cerebellum, basal forebrain, neocortex etc. [13]. It works as a neuromodulator agent in the brain, which can excite or inhibit the neurons. For years, it has been claimed that ACh has the crucial role in cognitive functions such as learning and short-term memory [3, 5, 14, 15]. However, the recent psychopharmacological and histological evidence support the idea that cholinergic system is an integral part of the attentional process [3, 6, 16].

Cholinergic system affects the attentional processes through two semi-separated but interacting processing mechanisms, as stated by Sarter et al. [5]. The first one is bottom-up (signal driven) processing or exogenous attention. The bottom-up processing is described as being under control of external signal such as sensory stimuli. Thus, it is known as stimulus-driven attention. It occurs immediately as a sudden loud noise or motion. It can unwillingly draws our attention [18]. It is mediated primarily by parietal lobe, temporal lobe and brainstem [19]. The second one is the top-down processing (goal-driven, endogenous). Observer's goals, desires or previous experiences play a vital role in the process and person intentionally allocates his/her attentional resources to a predetermined location or space [20]. The frontal lobe and basal ganglia

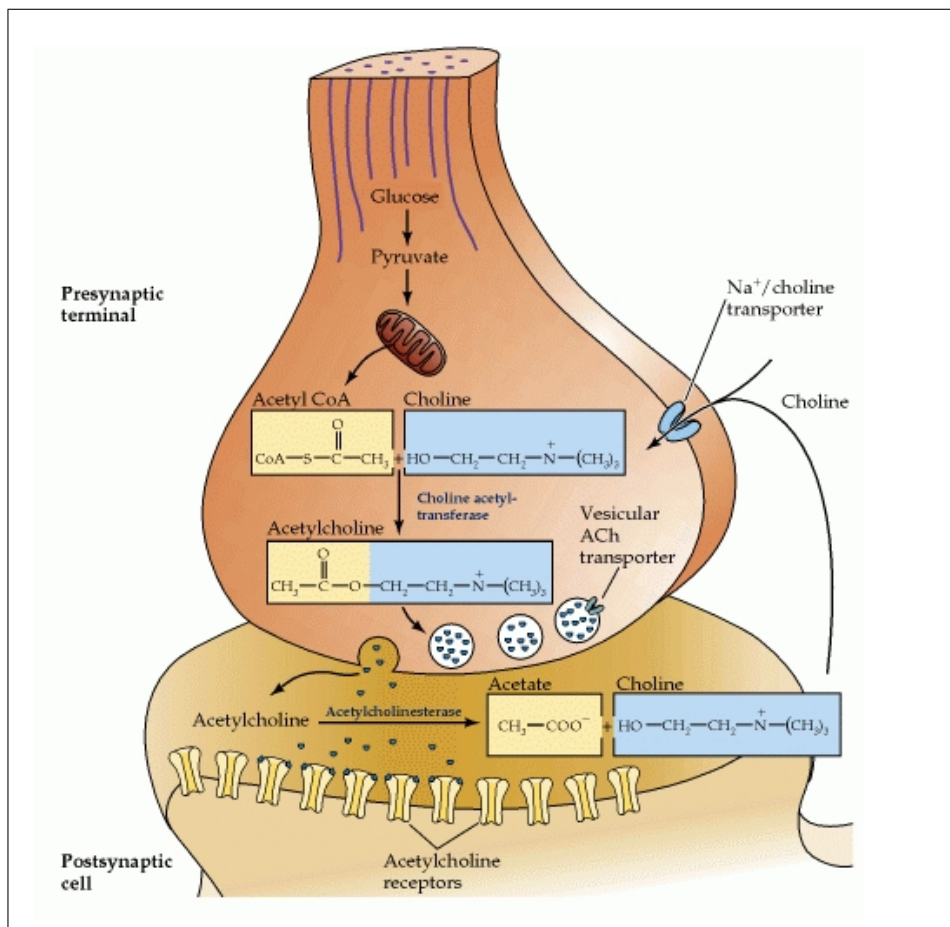


**Figure 2.1** Working system of the ACh in the synaptic cleft (Adopted from [17]).

primarily mediate the system as an executive function [21]. The cholinergic system can make selective attention easy by a general effect on "top-down" mechanism in parietal cortex especially in frontoparietal part [22] and via region-specific influences in perceptual areas of the sensory system.

The contribution of the cholinergic system to the attentional process is optimizing signal processing in particular in attention required contents. To do this, specific projections from the basal forebrain are necessary. Consequently, the encoding of information and processing of attention required tasks are enhanced by boosting the process of sensory input (bottom-up processing). These projections can be organized and adjusted by the prefrontal cortex impact on the basal forebrain as well. Thus, remote control of the cortex can be conducted by prefrontal cortex [4, 22–29].

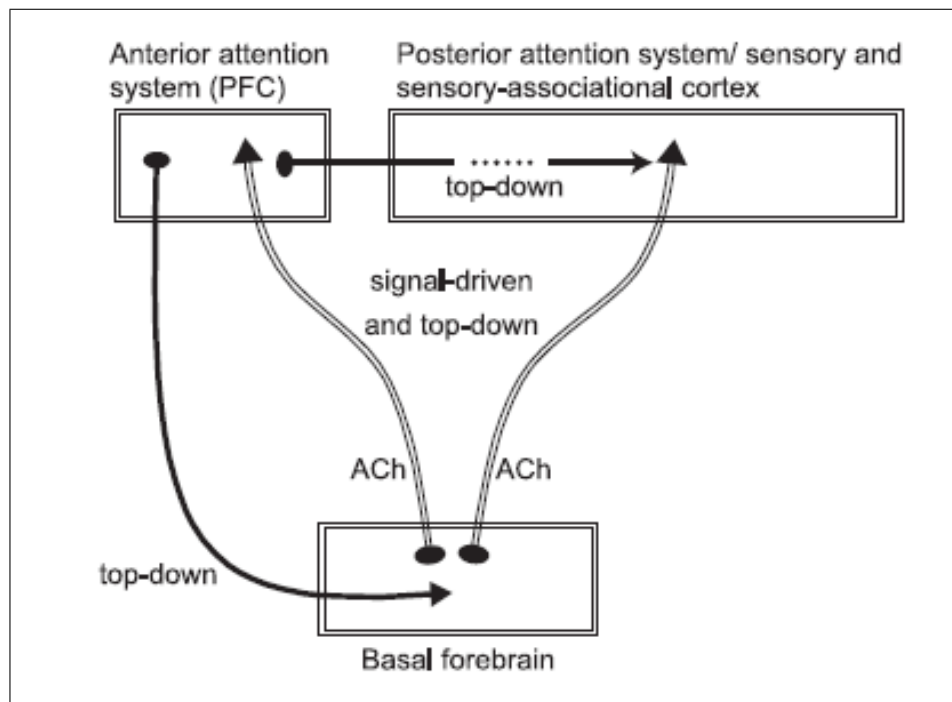


**Figure 2.2** Schematic diagram of posterior and anterior attention system and their elements [5].

The release of ACh is specific to the area and types of sensation, regardless of which mechanism (top down or bottom up) is used [30, 31]. For instance, in frontal cortex, thalamocortical connections are facilitated after olfactory, auditory and tactile stimuli and ACh release is elevated [32]. In somatosensory cortex, inputs (excitatory and/or inhibitory) from cortico-cortical connections are suppressed or facilitated by ACh receptors after tactile stimuli [32]. These discrepancies are more likely caused by the characteristics of receptors on the cell membrane. However, it can be interpreted from the pharmacological studies that the sensory input processing in attentional performance is regulated predominantly by ACh via the activity of nicotinic (nAChRs) and muscarinic (mAChRs) acetylcholine receptors in the cortex.

Classifications of the receptors were made according to different pharmacological properties of the molecules such as affinity and sensitivity. Sarter et al. demonstrated that intrinsic connections belong to top-down processing mechanism, which are excitatory or inhibitory, are regulated via muscarinic receptors whereas, sensory input processing is regulated by nicotinic receptors [5].

## 2.2 Cholinergic receptors

### 2.2.1 Nicotinic Receptors

Nicotinic receptors (nAChRs) are ligand-gated channels which are pentameric, nonselective cationic, and excitatory. It belongs to the Cys-loop receptor family [33]. These channels are proteins with a molecular mass of 290 kDa, and they have 5 subunits ( $\alpha$ ,  $\beta$ ,  $\gamma$ ,  $\delta$  and  $\varepsilon$ ) arranged symmetrically around a central pore (pentamer) [34] (see Figure 2.3). In vertebrates, 2 different subtypes of nicotinic receptors are defined based on their primary sites of expression; muscular subtypes and neuronal subtypes. Nicotinic receptors are expressed by sixteen genes. Five genes are responsible for encoding of neuromuscular type of nAChRs and the eleven genes are responsible for encoding of neuronal subtypes [35, 36]. This type is located postsynaptically and responsible for the contraction and relaxation of the muscles [33]. The neuronal subtypes of nAChRs are composed of the combination of nine different nicotinic receptor subunits;  $\alpha_{1,2,3,4,5,6}$  and  $\beta_{2,3,4}$  [37–39]. The all combinations can be seen in Figure 2.3 [40]. These receptors are abundant in the central nervous system on neuronal and non-neuronal cells such as glial, and endothelial cells. They are found in the layer I, III, IV and upper layer VI of cerebral cortex [41–44]. Clarke [41] and Sahin et al [45] demonstrated that presynaptically located nAChRs have direct role in thalamocortical transmission [46, 47]. nAChRs are also known to be located postsynaptically on interneurons [45]. They act as intermediary in the postsynaptic action of the ACh [43, 46]. Synaptic transmission of intracortical synapses are enhanced as well [45, 48–51]. Subunit composition of the nicotinic receptors are most probably the reason for the functional diversity of the nAChRs [52]. The nicotinic receptors have functionally significant two major subunits which are predominantly expressed subtypes in the mammalian brain. The  $\alpha 4\beta 2$  (high affinity nicotinic heteromeric acetylcholine receptors) and  $\alpha 7$  nAChRs (low-affinity nicotinic receptors) [36, 53].  $\alpha 7$  nAChRs are found especially in hippocampus and prefrontal cortex (PFC). It has role in neuroplasticity and memory functions in the hippocampus. In addition to the hippocampal role, it also has role in regulating working memory in the PFC [33]. The  $\beta 7$  nAChR subtype is responsible for the neuronal growth regulation, differentiation of neurons and formation of synapses during

development [54]. Nicotinic receptor activity increases in afferent connections. If it collaborates with muscarinic receptors, suppression occurs on intrinsic junctions. Thus, old information is suppressed while new information is amplified. Therefore, nicotinic receptors have an important role in enhancing certain part of memory phases [55].

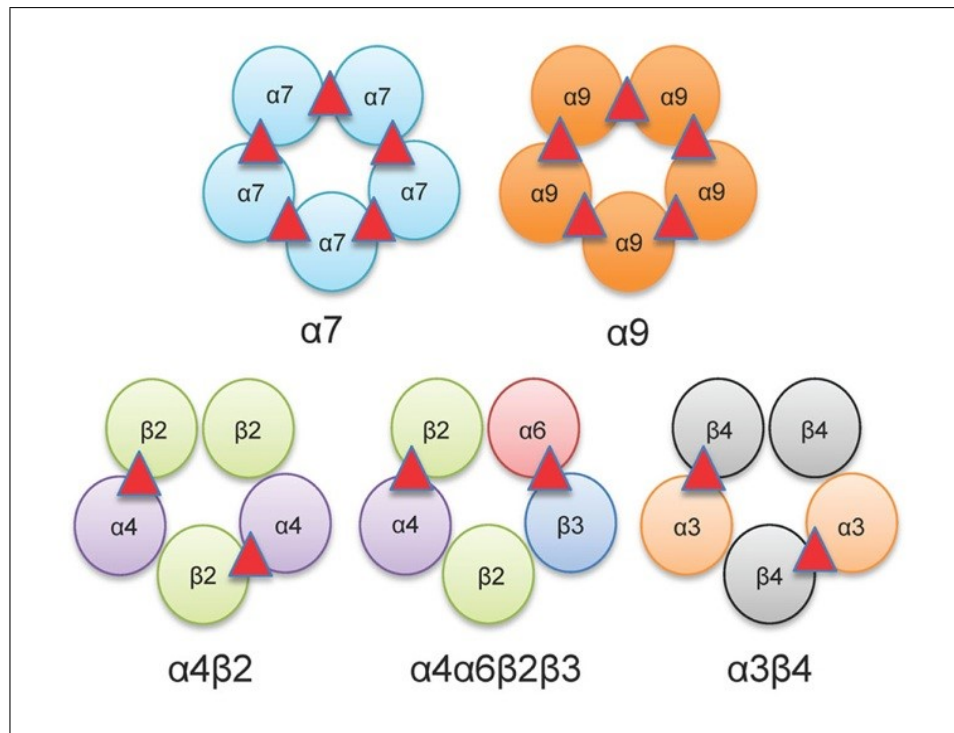


**Figure 2.3** Structure of nAChRs [40].

### 2.2.2 Muscarinic Receptors

mAChRs are G-protein coupled metabotropic receptors. They have received this name because it is sensitive to muscarine, which is a toxin obtained from mushroom. Using selective radioactive-labeled agonist and antagonist substances, five subtypes of muscarinic receptors have been identified (M1-M5) in mice and in human [56]. On the other hand, there are only four subtypes in rat; M1-M4 [57]. The structure of all four is shown in Figure 2.4 [40]. G protein family can be classified based on binding of  $\alpha$  subunit to G protein (i.e. Gq/11 and Gi/o). M1, M3 and M5 bind to Gq/11, while

M2 and M4 bind to Gi/o. Although M1, M2 and M4 are distributed throughout the cortex, expression of M4 is less than M1 and M2 [58].

When muscarinic receptor subtypes is compared to nicotinic receptor subtypes, much less is known about the action of the muscarinic subtypes in the brain [58, 59]. M1 receptor works both in exocrine glands and central nervous system (CNS). Neurophysiological studies in human and rat showed that M1 subtype is found in both postsynaptic and presynaptic sites of the neurons in CNS. M2 receptor is located in the heart (myocardium) in the peripheral nervous system (PNS). It is responsible for slowing the heart rate and decreasing the contractility of the atrium. The functional problems in the ion channel-M2 receptor system causes diseases such as Chagas disease. M2 can be found widely in the CNS as well. Generally, in the CNS it works as an inhibitory neuromodulator e.g. in caudate putamen. M2 subtype is located on the presynaptically and/or postsynaptically on the membrane [46]. Under electron microscopy investigation, it localized on axons terminals and dendrite spines [40, 60, 61]. M3 receptors can be found in lungs, blood vessels and urinary tract [62]. It is responsible for the regulation of saliva activity when the food intake starts. Growth hormone activity is regulated by M3 receptors. On the other hand, M3 is also expressed in CNS (hypothalamus, hippocampus etc.). M4 receptors are mostly found in the striatum in the CNS. In the Parkinson's disease, the key area is the striatum and the extensions of dopaminergic neuron onto the striatum decreases and muscular deficits. Thus, M4 receptor antagonists are used in the Parkinson's disease to reduce patient's tremors and rigidity of the muscles.

Studies with mAChRs agonists and antagonists to understand the role of the mAChRs in nervous system have already showed that mAChRs mediate several effects of ACh in the developing CNS. For example, effects of ACh is mediated by mAChRs on proliferation of astrocytes and oligodendrocytes, differentiation and survival of the cell in rat [54]. On the other hand, ACh has an inhibitory role through muscarinic receptors. This allows selection of particular information while suppressing others [63, 64]. In vivo studies indicate that some modulation of the cortical responsiveness

is mediated by the activation of mAChRs [65, 66]. It has been known that muscarinic receptor has several different effects on different cortical layers and cell types [67]. For example, studies conducted on brain slices show that muscarinic receptor activation has striking effect on the slow depolarization of the pyramidal cells in the cortex and this effect increases the spike response to excitatory signal [60]. It was determined that the combined blockade of nicotinic and muscarinic receptors has stronger impact than each receptor type blockade alone. However, the underlying mechanism still have not been identified [7, 61, 68]. The specific roles of these subtypes on the regulation of neuronal signal mechanism are not very clear.

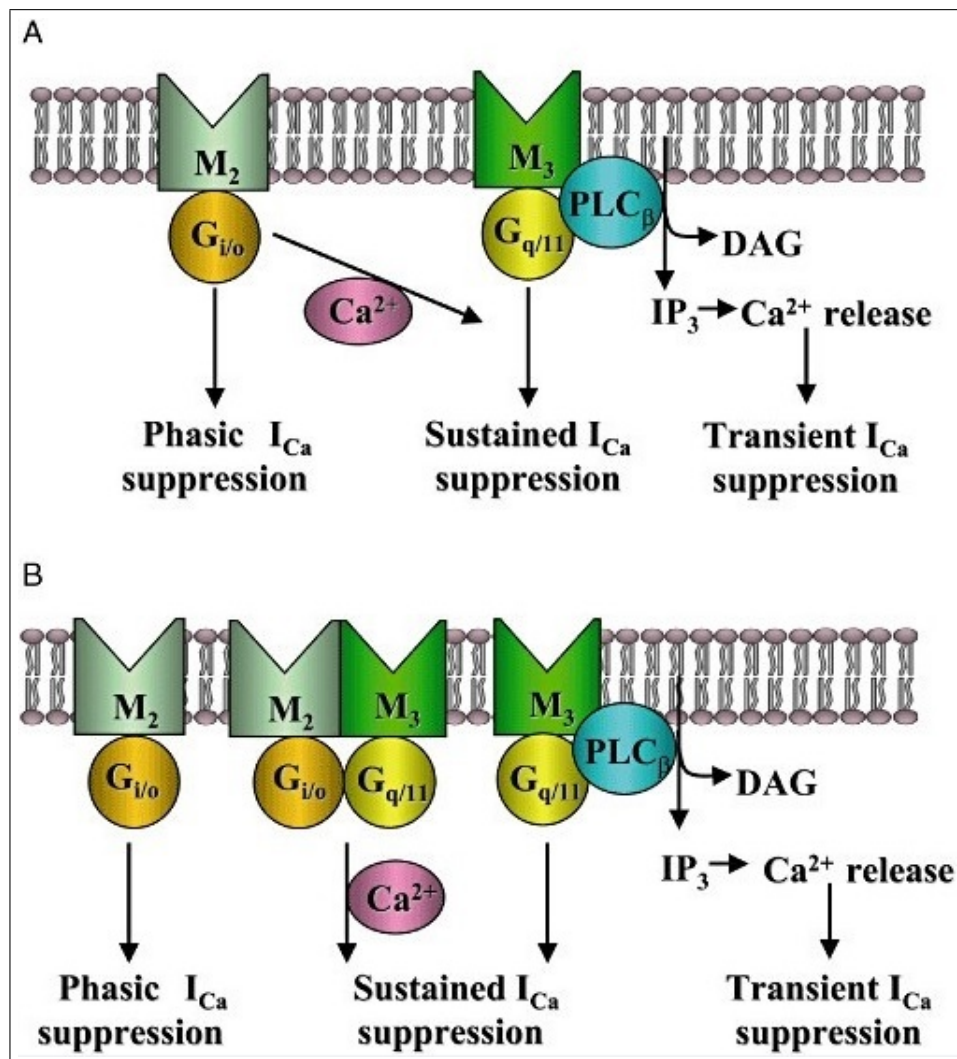
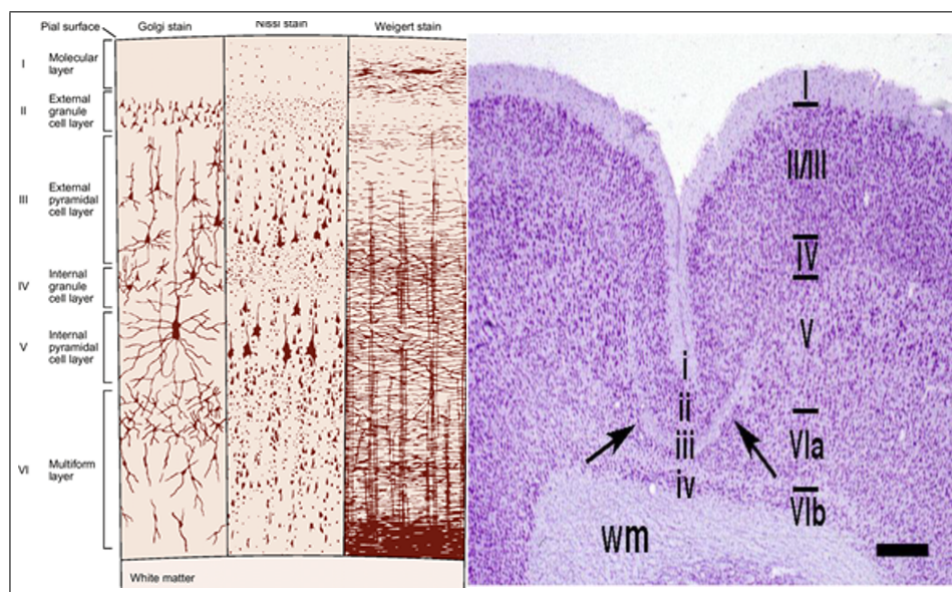


Figure 2.4 Structure of mAChRs (Adopted from [69]).

## 2.3 Cytoarchitecture of the Neocortex

The neocortex is the last evolved compartment of cerebral cortex in mammals. It constitutes the 90% of the cerebral cortex in human. It is the outer layer of the brain that covers the whole brain. It has convolutions called gyri and sulci. Neocortex is considered to be a significant progress that it is responsible for carrying out a huge number of 'higher' brain functions done by the nervous system such as consciousness, cognition, language, problem-solving, motor and sensory processing [40]. Different mammalian species have neocortices varying in shape, size, and neuron number [70].

Neocortex is approximately 1-4 mm thick and there are mainly 6 layers which are given in sequence going from the most superficial to the deepest level, Layer I to layer VI. The morphological and the functional properties of each layer in neocortex vary from one to other. The layers were initially distinguished on the basis of their appearance in Nissl stained sections, which is primarily sensitive to the density and size of neural cell bodies. The detailed columnar structure may be seen in Figure 2.5 [71].



**Figure 2.5** Detailed columnar structure of Neocortex [71].

Molecular layer I is also called plexiform layer, which is located closest to the pial surface of the brain. This layer has few neuron bodies. It contains many nuclei, which belong to glial cells, myelinated fibers and few neurons of granular and horizontal neurons of Cajal. It consists almost all axonal and dendritic branching [72]. External granular layer II, which is known as an outer granular layer contains small granular (Golgi type II cells) and pyramidal neurons. Granular type neurons are divided into two distinct types. One is Golgi type II with short axons that reach close to neuron body. Second, The Golgi type I has long axons reaching far from the body. Its axons go up to the cortical surface where it can make various axonal and dendritic connections. Layer III has moderate and large sized pyramidal neurons. Furthermore, there are some Martinotti (triangular or polygonal) and granular neurons. Afferent fibers projecting from thalamus, cortico-cortical connections reach layer III and IV. These synapse with both efferent cortical neurons and intercortical (granular, Martinotti and horizontal types) neurons. Internal granular layer IV mainly consists of Golgi type II and some small pyramidal neurons. It is an input layer with the layer II and receives inputs from the thalamus and other regions of cortex [73]. Internal pyramidal layer V contains large pyramidal neurons, few Martinotti and granular cells. Due to having huge pyramidal Betz cells in the motor cortex, this layer is also called Ganglionic layer V. The pyramidal neurons have (in Layer III and Layer V) apical and basal dendrites. Apical dendrites extend to superficial layers of the cortex while basal dendrites mainly remain within the layer. Fusiform layer VI contains almost all types of neurons such as Golgi type I and II, fusiform (spindle-shaped ascending dendrites), and Martinotti cells (long ascending axons). Many myelinated neuron fibers that come from and go to medulla are also located here. Extension of the dendrites of the large cells can reach to the layer I but small neuron's dendrites can reach only to layer IV. Layer VI cells' axons can extend to subcortical (e.g. thalamus) and cortical areas.

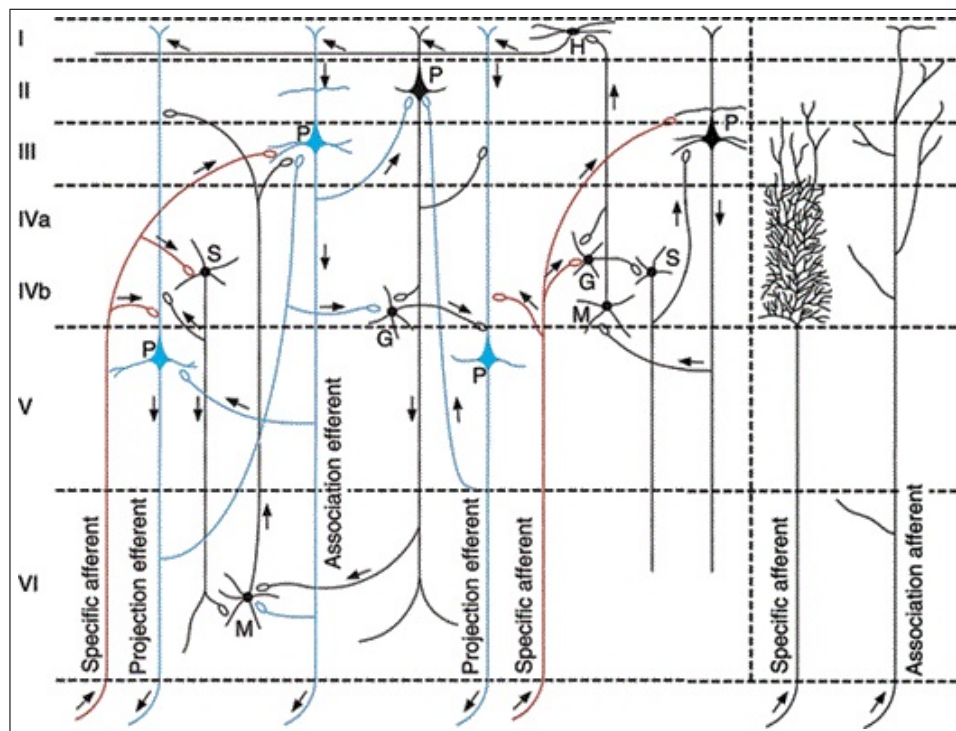


**Figure 2.6** Neural circuits in the cortex (G: granule cell, H: horizontal cell, M: Martinotti cell, P: pyramidal cell, S: stellate cell. The arrows in the figure shows the information flow)[73].

## 2.4 Localization of Cholinergic Receptors in the Cortex

In the literature, there are some studies used histological and immunohistochemical methods such as acetylcholinesterase (AChE) and choline acetyltransferase (ChAT) to visualize the ACh release and the projections of the neurons in the cortex [42],[74]. AChE is an enzyme responsible for hydrolysis of ACh at the synaptic cleft. Thus, it interrupts the cholinergic activity in the synapse [7]. It was used as the target of staining to visualize neurons which contains this enzyme. AChE staining results in a dense staining in layer I, IV and VI of somatosensory cortex of rat [7]. However, this method is not convenient to visualize cholinergic neurons and their projections since it has been proven that non-cholinergic neurons also have AChE. In the 1970s, specific monoclonal antibodies against ChAT have been used to visualize cholinergic neurons. ChAT is an enzyme responsible for the biosynthesis of ACh. Therefore, ChAT is a direct marker for cholinergic neurons. ChAT-positive dotted structures and varicose fibers are presented through all layers of the cerebral cortex. Many of these fibers which are vertically oriented create a meshwork impression to several cortical layers. Houser

et al. [42] showed that cholineceptive neurons are seen within the cerebral cortex and are located from layer II to VI. The cholinergic innervation is the highest in the deeper layers (specifically layer V) compared to superficial layers (e.g. layer II and III) [74]. Small sized neurons (average of somata diameter is 14- 18/  $\mu m$ ) and multipolar shaped neurons are rarely seen [42, 75]. Although staining of ChAT is more specific to label cholinergic neurons, both AChE and ChAT do not give any information about receptor types and/or their laminar distributions. In other words, to understand the functional effect of the innervation, one must study the target neurons which express cholinergic receptors. Therefore, labeling of cholinergic receptors with antibodies allows the researchers to detect the location and to quantify the distribution of these receptors. In study of Zee et al [7], immunofluorescence labeling revealed that individual cholineceptive cells within cortex express enhanced levels of both nicotinic and muscarinic receptor types. The highest number of cells with cholinergic receptors is observed in layer V of parietal cortex. In layer II and III, it is highly presented as well. Receptor density decreases in the order of layer II, III, VI and layer IV [7]. However, there is no detailed information about the distribution of muscarinic and nicotinic receptors in different layers of the somatosensory cortex.

## 2.5 Aim of the Study

In the previous studies, the general distribution of cholinergic receptors in parietal cortex and motor cortex was already shown [7]. However, the detailed distribution of the muscarinic and nicotinic ACh receptors was not investigated in particular areas in the somatosensory cortex, that is to say barrel cortex. In this thesis, it is hypothesized that the distribution of cholinergic receptors is not homogenous throughout the primary somatosensory cortex (SI), because the projection densities from other brain regions to different representations (i.e. barrel field and hindlimb area) in SI are different. The novelty of this study is that it provides information about the distribution of M2 in the barrel field (S1BF) and hindpaw representation of SI cortex (S1HL) (anterior part of the parietal lobe) in each cortical layer. With the result of the thesis, we aim to understand anatomical basis of attentional modulation in the sensorimotor

areas of the rat cortex. Additionally, the results of the study will be used for creating computational models of vibrotactile neurons in rat cortex.

### 3. MATERIALS AND METHODS

#### 3.1 Animals

All procedures of the experiment were approved by Boğaziçi University Institutional Ethics Committee for the Local Use of Animals in Experiments (BÜHADYEK). These rats were previously used in the electrophysiology experiments performed in our laboratory. Ten adult (3 Female, 7 Male) Wistar albino rats were used in the Nissl staining. Seven adult (2 Female, 5 Male) Wistar albino rats were used for EtBr staining and immunohistochemistry (IHC). The rats were anesthetized with ketamine (65 mg/kg) and xylazine (10 mg/kg) intraperitoneally (IP) before transcardial perfusion.

#### 3.2 Fixation and Brain sectioning

In order to preserve tissue well and prevent from autolysis and decay, the brain was fixated by transcardial perfusion. Saline solution (0.9% NaCl) was used to clean the blood out of the tissues first and then 4 % paraformaldehyde (PFA) was used to fixate the tissues in a gravity-feed system. Post-fixation was made with neutral buffered paraformaldehyde (NBPFA) / Sucrose solution (20% sucrose in 4% paraformaldehyde). When the brain sank in solution, the brain was ready to be sectioned. The brain was sectioned in 50  $\mu m$  thickness by using a vibratome (Leica VT1000S-vibration frequency: 30Hz, cutting speed: 0.25 mm/s). Sectioning was done in phosphate buffered saline (PBS) solution to keep the tissue wet. Tissue sections were placed onto slides coated with gelatin and were left in the room temperature for 12 to 18 hours for desiccation, which is carried out to dehydrate the tissue physically.

### 3.3 Nissl Staining

First, alcohol series were performed for dehydration, demyelination, and rehydration (70%, 95%, 100%, 95%, 70%, and 50%). Then, slides were rinsed in distilled water ( $dH_2O$ ) which is followed by staining with Cresyl Violet for 4 to 5 minutes. To remove excessive dye, slides were washed with two changes of distilled water. To dehydrate the tissue, sections were rinsed in 95% and 70% alcohol for 5 minutes. Slides were placed in a differentiation solution (acetic acid + 95% alcohol) to adjust the color of stain. Dehydration was continued with 95%, 100% alcohol, one minute each. Lastly, slides were held in xylene for 3 minutes to clear the tissue. After clearing, slides were allowed to dry in room temperature and coverslipped with Entellan (Merck). All stages of the protocol was shown below in Figure 3.1.

### 3.4 Immunostaining

12 sections were prepared from each animal to investigate the brain areas. Prepared slides were selected for two different staining procedures EtBr and immunostaining for M2 receptor. The 1<sup>st</sup> and 7<sup>th</sup> sections were selected for EtBr staining. From 2<sup>th</sup> to 4<sup>th</sup> and 8<sup>th</sup> to 10<sup>th</sup> were chosen for IHC-M2. The other sections (5<sup>th</sup>, 6<sup>th</sup>, 11<sup>th</sup>, and 12<sup>th</sup>) were selected for negative control. The 5<sup>th</sup> and 11<sup>th</sup> were used for secondary antibody control in which the secondary antibody is not added to sections while the other steps of the protocol are applied as others. On the other hand, the 6<sup>th</sup> and 12<sup>th</sup> sections were used for primary antibody control in which the primary antibody is not applied.

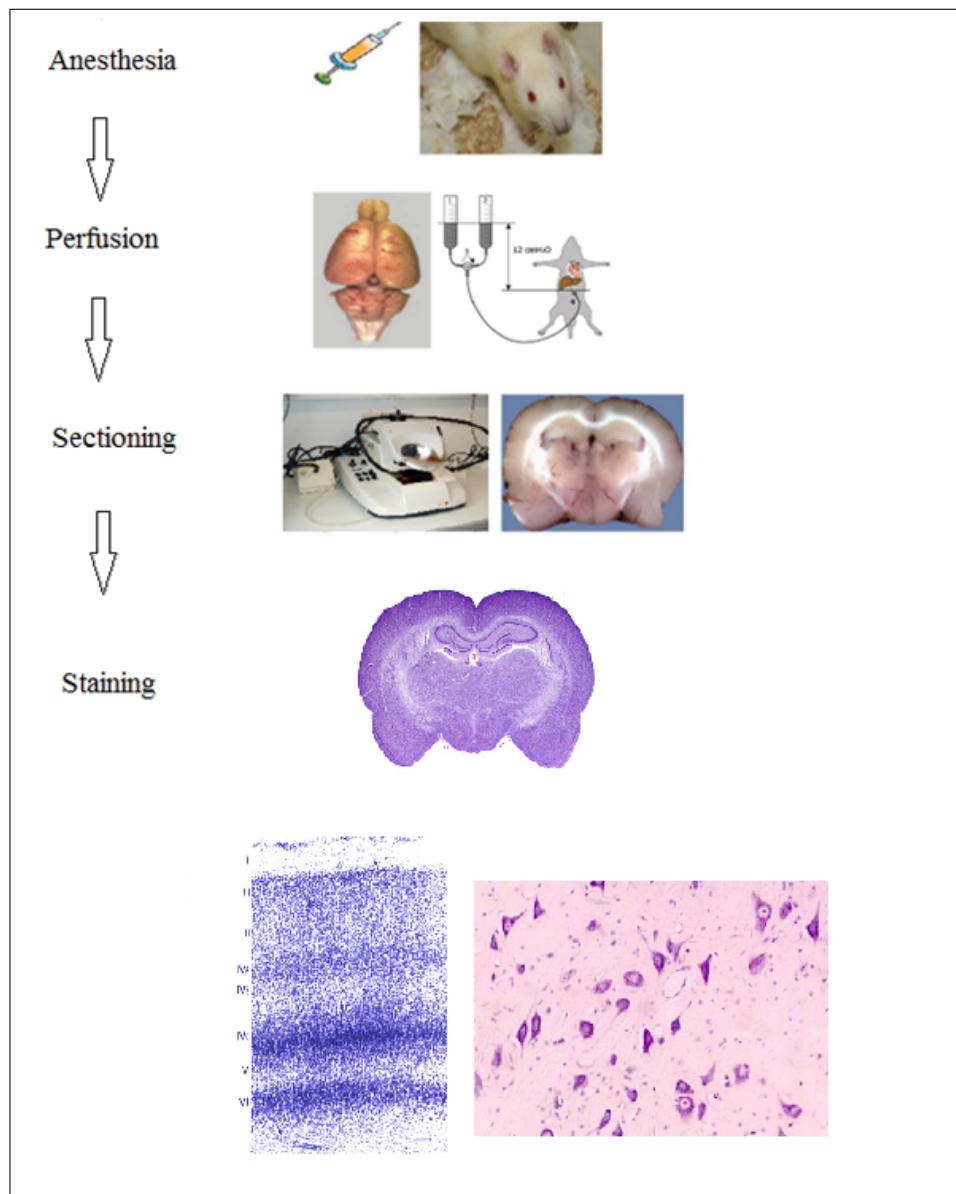


**Figure 3.1** Flow diagram of Nissl Staining.

### 3.5 Counterstaining for Immunofluorescence

Layer thicknesses and the total number of neurons in the S1HL, S1BF and M1 were initially determined on slides stained with EtBr. EtBr was chosen because it can be used as a long lasting tissue dye and can preserve the color of stain from fading. EtBr has an excitation wavelength around  $\sim 518$  nm and emits the light at a wavelength of  $\sim 605$  nm. Thus, the neurons stained with EtBr were visualized under green light (excitation) with a filter detecting orange light (emission). Excitation and emission

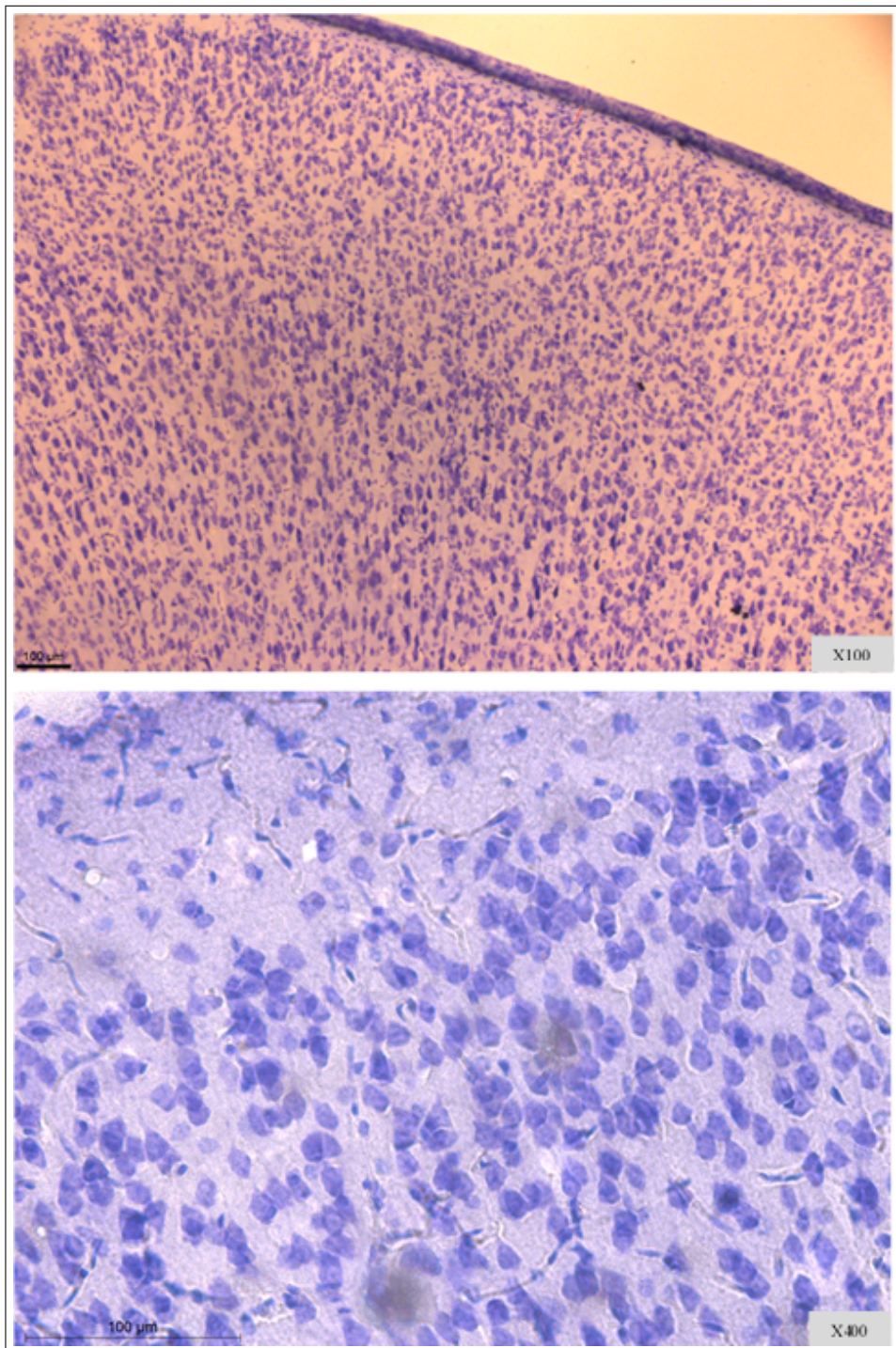


**Figure 3.2** Pictures with different magnifications (X100 and X400).

spectra for EtBr is shown in Figure 3.3.

After the brain sank in the neutral buffered paraformaldehyde (NBPFA)/Sucrose solution (20% sucrose in 4% paraformaldehyde) (post-fixation), brain was washed 6 times

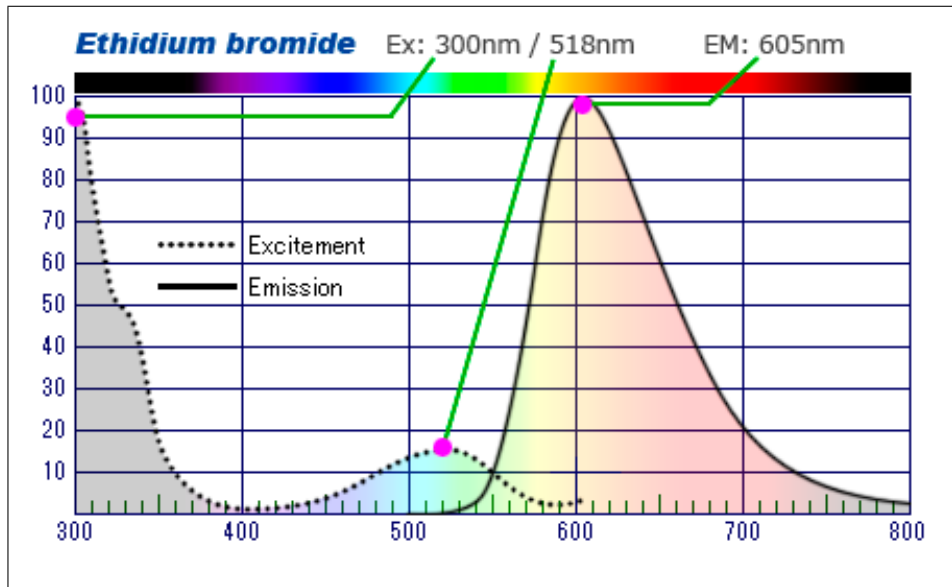


**Figure 3.3** Excitation and emission spectra for Ethidium Bromide (EtBr) [76].

in phosphate buffer (PB) that contains Triton X (PBTx) which is used as a detergent that permeabilizes the tissue membrane. After rinsing with PBTx with 10% normal goat serum (NGS) (PBTxg), sections were placed onto gelatin-coated slides to dry. Air dried sections were rehydrated in distilled water for 2 minutes. Then, sections were exposed to EtBr solution for 1 minute. They were rinsed in PB for 2 minutes. In the final step, they were washed in distilled water and mounted using Fluoroshield™ (Sigma-Aldrich) which is used to protect the tissue from light. The samples were maintained at +4 °C. The cortical neurons stained with EtBr are shown in Figure 3.4.

### 3.6 Antibody staining

In order to detect the M2 receptor complexes on the neurons of the sensorimotor areas of the rat cortex, mouse monoclonal anti-mAChR2 (IgG1) (ThermoFisher Scientific: MA3-044) was used as the primary antibody which is specific to rat muscarinic acetylcholine M2 receptor complexes. Goat anti-mouse IgG H+L (Alexa Fluor 594®) (ThermoFisher Scientific: A-11012) was used as conjugated secondary antibody. Its excitation wavelength is 591 nm and emission wavelength is 614 nm. Thus, the M2

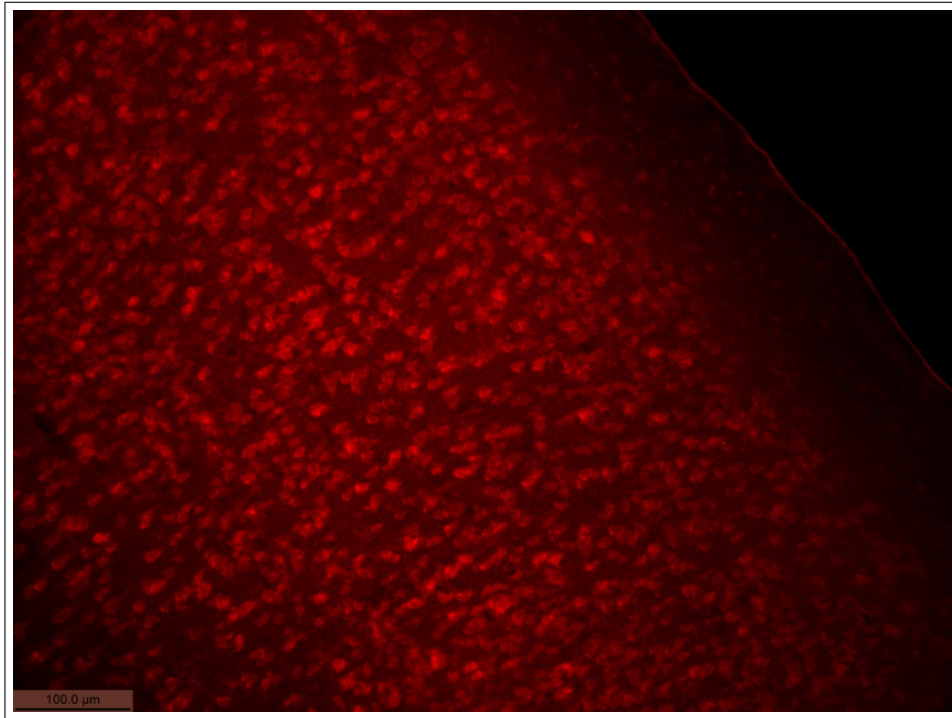


**Figure 3.4** A sample of EtBr (rat 218 sld7- s1bf 2).

complexes were visualized under green light. The excitation and emission spectra for Alexa Fluor 594 is shown in Figure 3.5.

After the brain sank in the neutral buffered paraformaldehyde (NBPFA)/Sucrose solution (20% sucrose in 4% paraformaldehyde) (post-fixation), brain was washed 6 times in PBTx. Sections were blocked with NGS. After blocking with 10% goat serum for an hour, the sections (from 2<sup>nd</sup> to 5<sup>th</sup> and from 8<sup>th</sup> to 10<sup>th</sup>) were incubated in 150  $\mu$ L primary antibody solution (diluted 1:250 in PBTx) for 24-48 hours in a humid box within the refrigerator at 4 °C. The sections were washed in PBTx for 3 times (each 30 min). Then, the sections were incubated in 150  $\mu$ L secondary antibody solution (diluted 1:50 in PBTxg) for 12-24 hours in a humid box within the refrigerator at 4 °C in the dark. The sections were rinsed 3 times (with at least 30 min/rinse) in different rows filled each time with 1.5 mL fresh PB. In the final step, to lower background staining, all samples, including controls, the sections were rinsed 2 times (each 15 min) in 4mM sodium carbonate solution. After that, sections were placed onto the gelatin-coated slides. For preserving fluorescence of the samples, Fluoroshield (Sigma-Aldrich) was

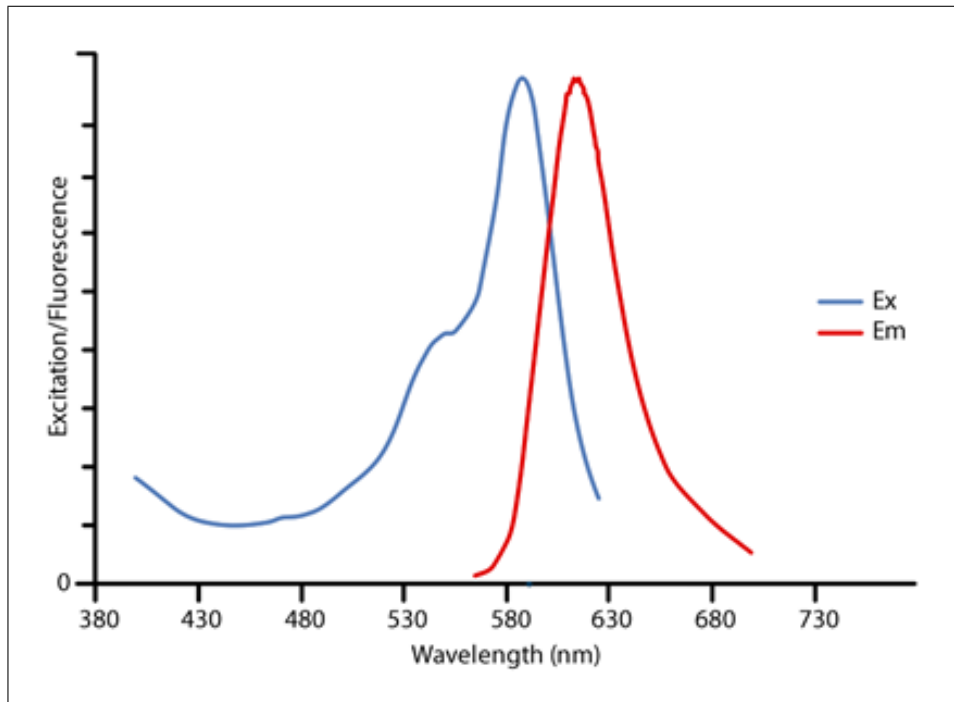


**Figure 3.5** Excitation and emission values of Alexa Fluor 594 [77].

used as mounting medium. Specimen slides were stored in the refrigerator and away from light at all times.

### 3.7 Cell Counting

Firstly, the appropriate filter cube (I3) was used to study autofluorescence in the tissues. Then, the filter N2.1 was used to immunostaining by using overlaid images. A specimen slide on the stage is positioned. The Leica software is used for all tissue monitoring and measuring steps.

In order to determine a midline through the brain areas (M1, S1HL, S1BF) shown in Figure 3.6, a normalization procedure is required. Due to the fixation of the tissue and variability among subjects the coordinates for locating the area boundaries were normalized according to Paxinos & Watson atlas [78]. Area boundaries were determined according to following equation. According to Paxinos & Watson atlas, hemispheric width (Figure 3.6) is given as 7 mm and midline distances for each area

are given as 1.36 mm, 2.60 mm, and 6.10 mm for M1, S1HL, S1BF, respectively. After the hemispheric width in subject were measured, normalized midline distance for each area is calculated. For example,

For M1

Hemispheric width in atlas (7 mm)                      Midline distance in atlas for M1 (1.36 mm)

Measured hemispheric width in subject      Normalized midline distance for M1 (x)  
(HW)

$$x = HW * 1.36 / 7$$

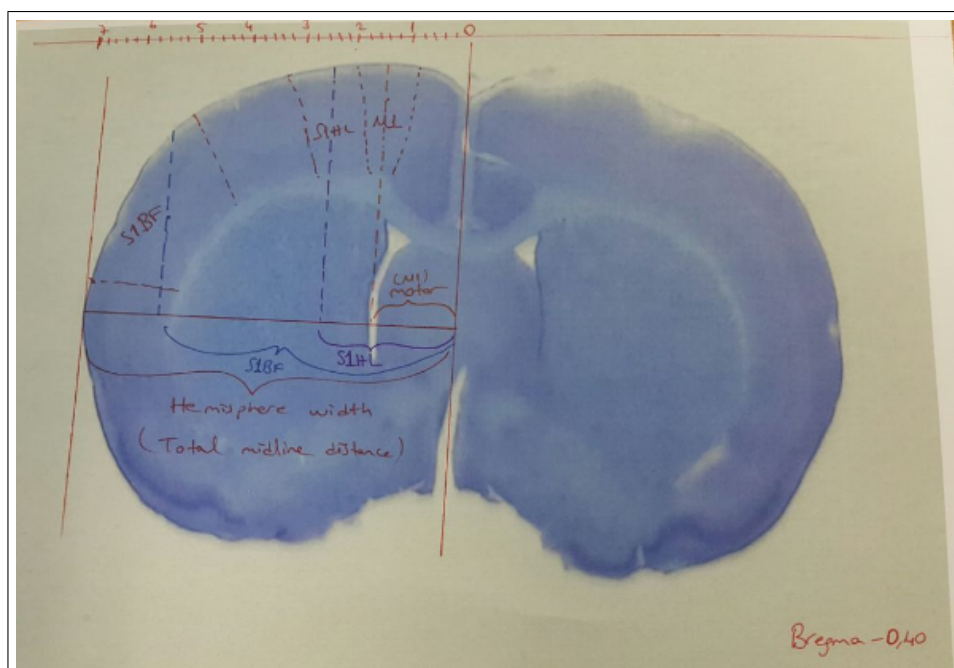


**Figure 3.6** Schematic showing the hemispheric width boundaries as well as the midline distance measurements in for each area.

The width (600  $\mu m$ ) of the counting area was identified by inserting borderlines on images. Annotations and measurements were performed on the Leica LAS software. ImageJ was [79] was used to count the cell. In immunofluorescence, we looked for cells labeled with the fluorophore, and not those with only autofluorescence. Hence, overlaid shapes didn't count as a M2RC due to the autofluorescence. M2RC are not very smoothly shaped. Thus, we didn't count the smooth shapes as receptor complexes, as well. Except them, we marked other shapes as a M2 receptor complex.

## 3.8 Statistical Analysis

### 3.8.1 Nissl stained data

Layers were identified based on cytoarchitecture reference. The thicknesses of the layers were measured in Leica software the following cortical areas within the neocortex: M1, S1HL and, S1BF. Mean, standard error and standard deviation were calculated for each layer thickness in a given cortical area. One-way ANOVA was conducted to determine whether the total cortical thickness varies across the areas and two-way ANOVA was used to find whether there are any effects due to particular layer and cortical area. SPSS Ver 22 (IBM Corp., Armonk, NY, USA) was used to do all statistical analysis. Any significant interactions were further studied with post hoc t-test.

### 3.8.2 Immunostained data

The average layer thicknesses ( $T$ ) from Nissl stained sections were used to determine layer boundaries in immunostained cell count analysis. The number of counted M2 receptor complexes were defined as  $N$  within a given cortical layer and area. The density of M2 receptor complexes was defined as the  $D = N / T$ .

Normalized number of M2RC according to total number of cells in a layer was defined as  $C = N/N_{\text{tot}}$ .  $N_{\text{tot}}$  is the total number of cells in a given cortical layer and area which is determined in EtBr stained sections.  $N$ ,  $D$ , and  $C$  were used as dependent variable in statistical analysis in SPSS. Two-way was used for each dependent variable with factors of cortical area (M1, S1HL, S1BF) and cortical layer (I, II, III, IV, V, VI).

## 4. RESULTS

### 4.1 Nissl Staining

Morphometric measurements were carried out on brain sections from ten Wistar Albino rats and the results are summarized in the Table 4.1. To find the thickness of each layer in a given subject, four measurements were performed on serial sections and they were averaged. Table 4.1 shows subject averages and standard errors. The layers were found for three brain areas primary motor cortex (M1), hindlimb area of somatosensory cortex (S1HL) and barrel cortex (S1BF). Additionally, total thicknesses were also measured. Sample measurements for each area are shown in Figure 4.1, 4.2, and 4.3.

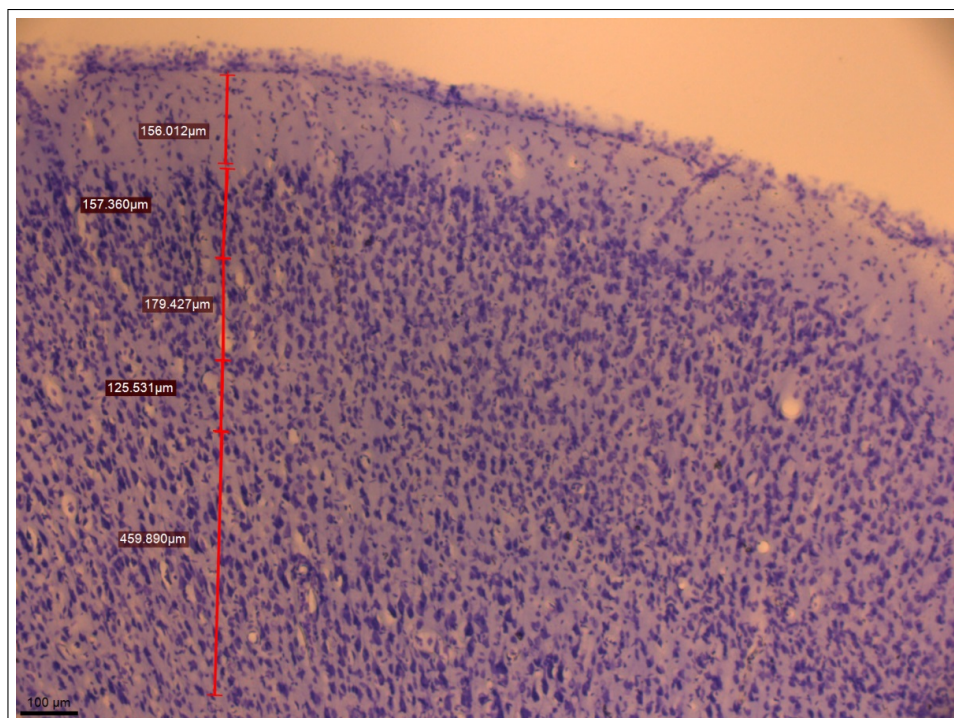


**Figure 4.1** Nissl staining for measuring the length of M1 in Neocortex.

According to one-way ANOVA result, there were no statistical difference in

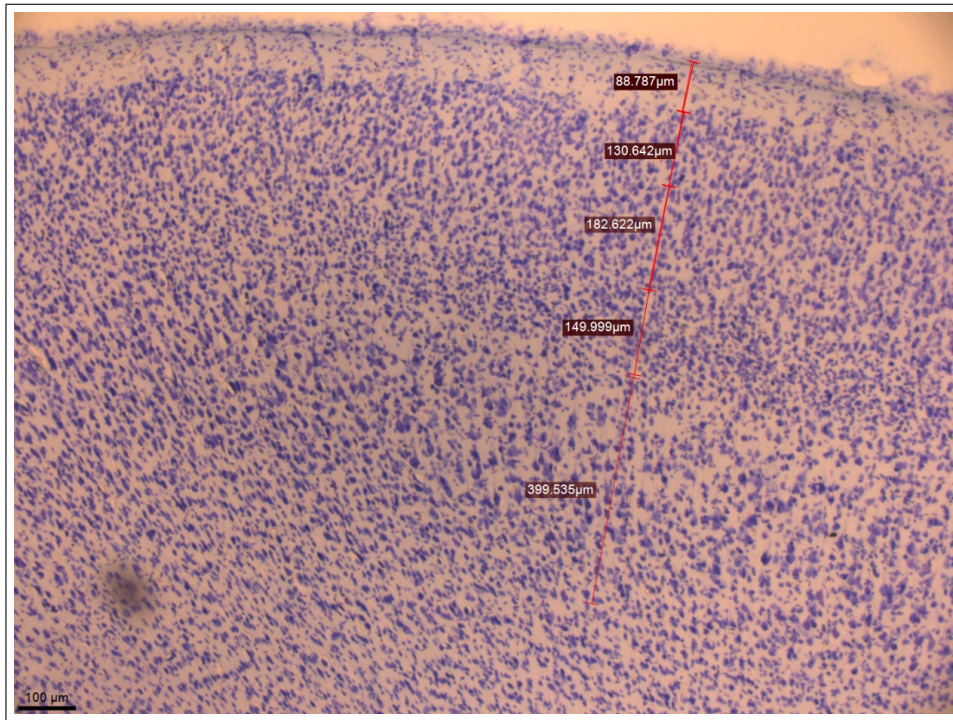


**Figure 4.2** Nissl staining for measuring the length of S1HL in Neocortex.

total thickness between brain areas tested ( $p=0.38$ ). The total thickness of M1 is  $1663.76 \pm 68.94 \mu m$ , while of those in S1HL and S1BF are  $1635.1 \pm 69.76 \mu m$  and  $1765.57 \pm 68.14 \mu m$ , respectively. Bar graph of total thickness for each area is shown in Figure 4.4.

Two-way ANOVA results shows that there are significant differences regardless of different brain area ( $p < 0.001$ ). Although there were no significant differences between areas as a main effect ( $p=0.11$ ), there was a significant layer and cortical area interaction. ( $p < 0.001$ ). To investigate whether there is interaction between layers and cortical areas, one-way ANOVA was performed for each layer. Paired post-hoc t-test was conducted on the layers, which have statistically significant results, to show the interactions between the cortical areas. According to the post hoc t-test results, there was no effect of brain area on layers I and VI. (Figure 4.5). However, there were significant differences between area in layers II, III, IV, V ( $p < 0.005$ ). Layers II, III and IV are thicker in S1BF compared to other two areas. On the other hand, layer V has lower thickness in S1BF compared to S1HL and M1 as seen Figure 4.5.

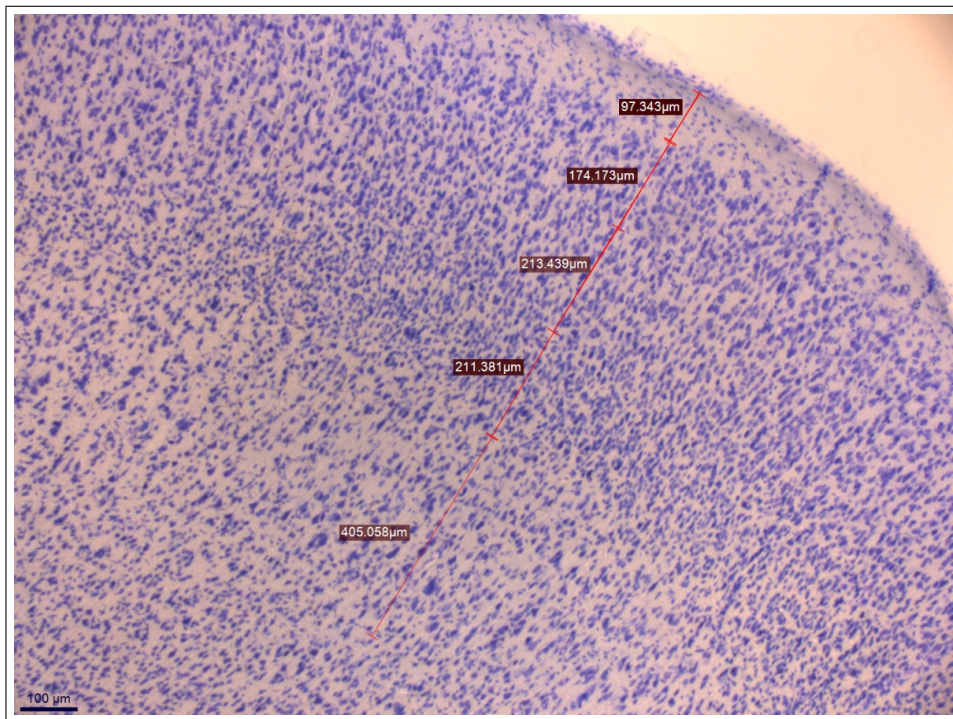


**Figure 4.3** Nissl staining for measuring the length of S1BF in Neocortex.

## 4.2 Muscarinic receptor M2 staining

M2RC and total number of cells in each layer were counted from seven Wistar Albino rats. Layer boundaries were determined by Nissl sections as described in previous sections. For each area of interest (M1, S1HL and S1BF), two slides for EtBr staining and two slides for M2 staining were used. Representative counted samples were shown in figures below for both EtBr staining (Figure 4.6 to 4.8) and M2 staining (Figure 4.9 and 4.10). Average number of M2RC in a layer ( $N$ ), density of M2RC with respect to layer thickness ( $D$ ), and normalized M2RC per total number of cells ( $C$ ) are given in Table 4.2 (See Appendix A for data from each rat). In order to study the effects of cortical layers and brain areas, two-way ANOVA was performed for all dependent variables described ( $N$ ,  $D$ , and  $C$ ). The results showed significant main effects of layer on  $N$ ,  $D$ , and  $C$  ( $p < 0.001$ ,  $p = 0.002$ ,  $p = 0.053$ , respectively). Area and layer interaction

**Table 4.1**  
The average layer thicknesses measured from different cortical areas.

Layer Thickness ( $\mu m$ ) Mean $\pm$ Standard Error	CORTICAL AREA		
	S1HL	S1BF	M1
<b>I</b>	97.31 $\pm$ 15.09	75.27 $\pm$ 9.96	96.28 $\pm$ 13.29
<b>II</b>	128.2 $\pm$ 10.15	175.2 $\pm$ 6.53	109.17 $\pm$ 9.74
<b>III</b>	155.71 $\pm$ 11.61	213.76 $\pm$ 9.86	132.96 $\pm$ 10.21
<b>IV</b>	174.57 $\pm$ 9.58	210.37 $\pm$ 13.44	118.55 $\pm$ 7.38
<b>V</b>	415.62 $\pm$ 22.78	371.77 $\pm$ 15.04	465.01 $\pm$ 30.14
<b>VI</b>	663.67 $\pm$ 33.6	719.19 $\pm$ 29.85	741.75 $\pm$ 35.07
<b>Cortex Thickness</b>	1635.1 $\pm$ 69.76	1765.57 $\pm$ 68.14	1663.76 $\pm$ 68.94

was also found for N ( $p < 0.001$ ). However, area did not have a main effect on all three variables. Lowest average number of M2RC (N) was observed in layer I for all brain areas. Layer V and VI in M1 have high number of M2RC (N) compared to S1HL and S1BF, whereas the average number of M2RC (N) was lower in layer II, III, IV in M1 (Figure 4.11). Despite being not statistically significant, S1BF has highest number of M2RC (N) especially in layer II, III and IV. When M2 receptor density was calculated by dividing number of M2RC by layer thickness (D), the highest values was observed in layer II and III for all areas. There was neither significant differences between areas nor any interaction between layer and area for D. The lowest density was observed in layer VI (Figure 4.12). In addition to these analyses, the relative number of stained M2 receptor was quantified by dividing number of labeled cells by the total number of cells (C) in each layer. There were significant differences between layers for C. Because the different sections were used for counting the total number of cells, the C measure was not reliable for layer I (Figure 4.13). Layer IV had marginally main significant effect on C. In general, layer II and III has highest M2RC/cell whereas layer VI had the lowest. There were no significant differences between cortical areas except layer IV in M1 where higher number of M2RC/cell was observed (Figure 4.13). Layer was also significant main effect ( $p = 0.05$ ). Layer II and III have highest M2RC/cell ratio whereas layer VI has the lowest.

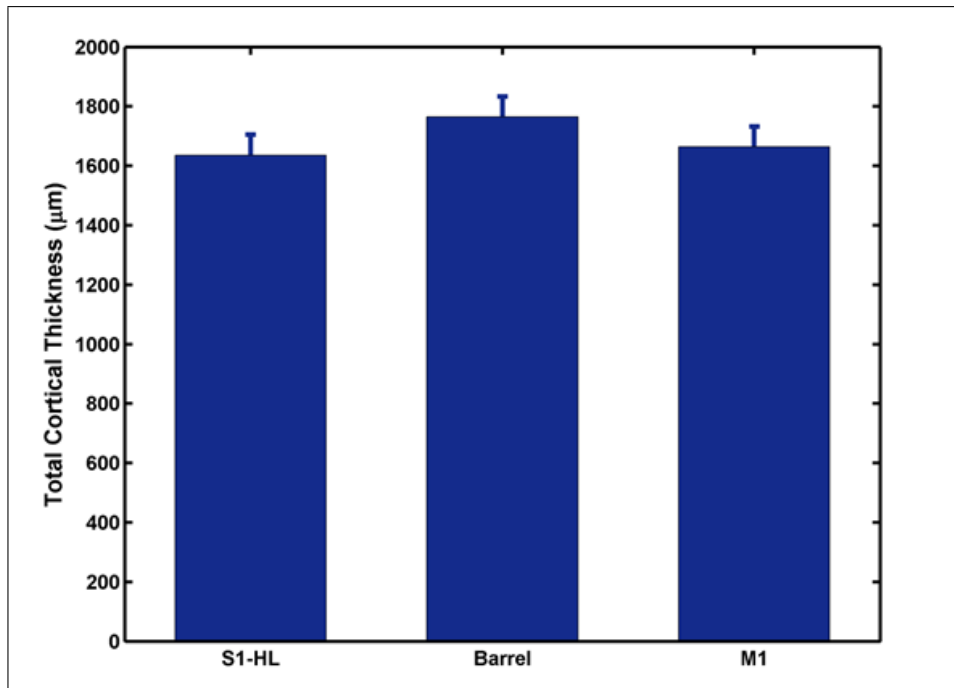


**Figure 4.4** Total thickness of the layers in relevant areas (M1, S1HL and S1BF) (Error bars are indicated in SEM).

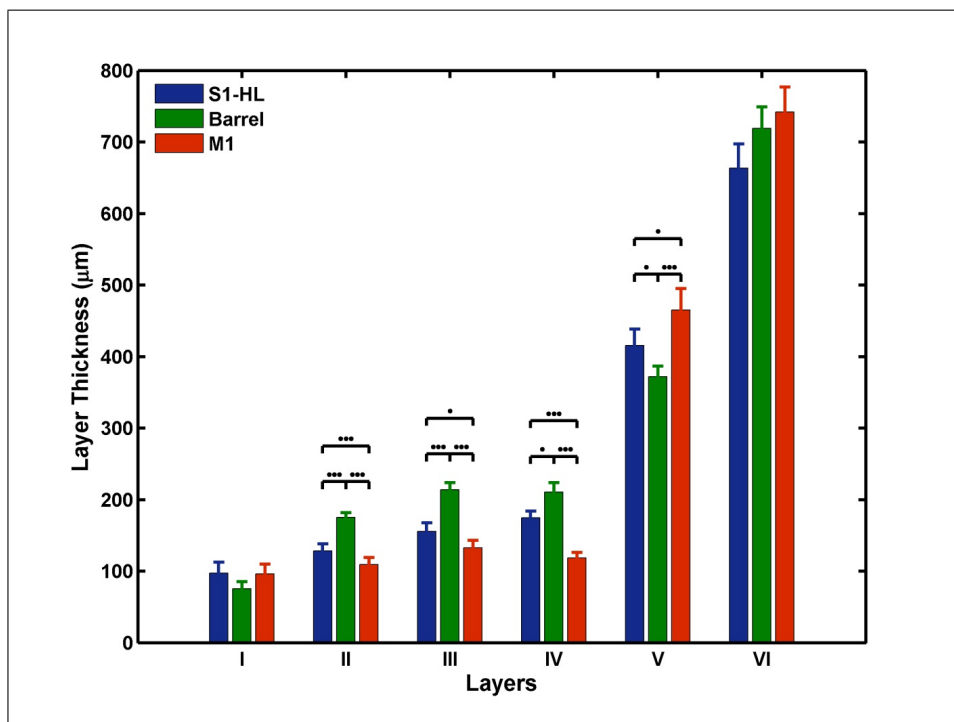


**Figure 4.5** The thickness of layers in M1, S1-hind leg and Barrel cortex (Error bars are indicated in SEM, p-values denotes  $** < 0.05$ ,  $*** < 0.005$ ).

**Table 4.2**

Average number of M2RC (N), average number of M2RC per mm thickness (D) and average number of M2RC per total number of cells (C) for each area (M1, S1HL, and S1BF).

<b>N (#)</b>	<b>Layer I</b>	<b>Layer II</b>	<b>Layer III</b>	<b>Layer IV</b>	<b>Layer V</b>	<b>Layer VI</b>
<b>M1</b>	20.56	142.66	148.97	135.00	359.49	309.21
<b>S1HL</b>	28.85	145.95	170.13	160.33	234.81	187.76
<b>S1BF</b>	11.21	165.63	196.77	202.14	212.06	237.76
<b>D (#/mm)</b>	<b>Layer I</b>	<b>Layer II</b>	<b>Layer III</b>	<b>Layer IV</b>	<b>Layer V</b>	<b>Layer VI</b>
<b>M1</b>	198.80	1200.76	1004.53	930.96	650.54	373.49
<b>S1HL</b>	320.39	1022.61	959.78	747.97	537.86	291.33
<b>S1BF</b>	169.14	1062.11	1070.79	761.26	542.31	353.56
<b>C (#/#<sub>tot</sub>)</b>	<b>Layer I</b>	<b>Layer II</b>	<b>Layer III</b>	<b>Layer IV</b>	<b>Layer V</b>	<b>Layer VI</b>
<b>M1</b>	1.68	0.81	0.66	0.56	0.51	0.24
<b>S1HL</b>	1.62	0.74	0.71	0.37	0.41	0.19
<b>S1BF</b>	0.64	0.60	0.52	0.39	0.39	0.23

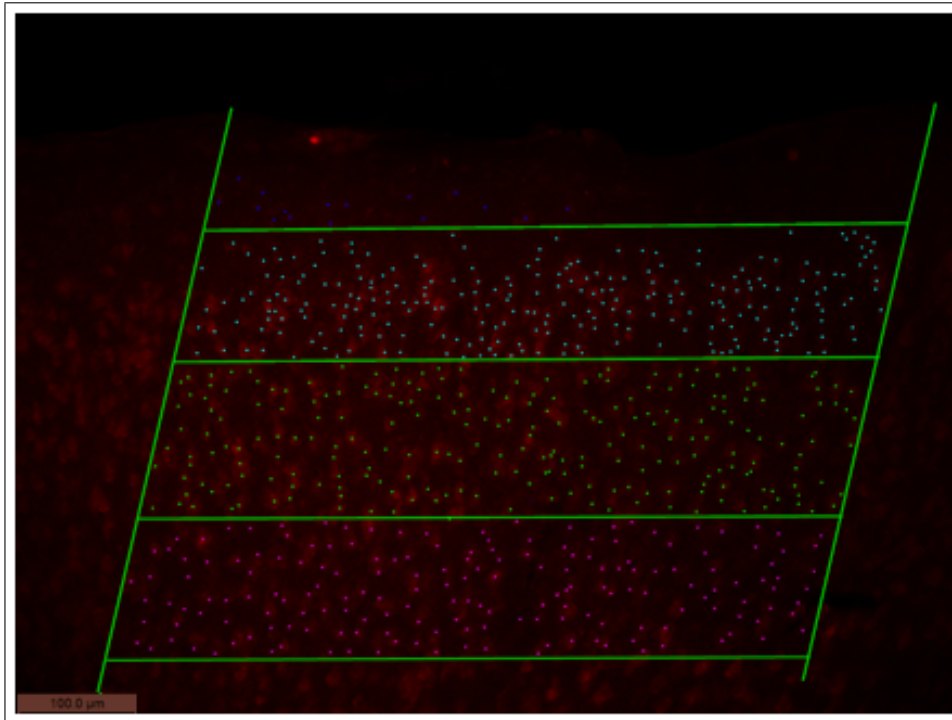


**Figure 4.6** EtBr staining for quantifying the total number of cells in M1. Horizontal green lines indicate layer boundaries. Green small dots indicate counted cells (Rat 217-slide 1-Magnification x20).

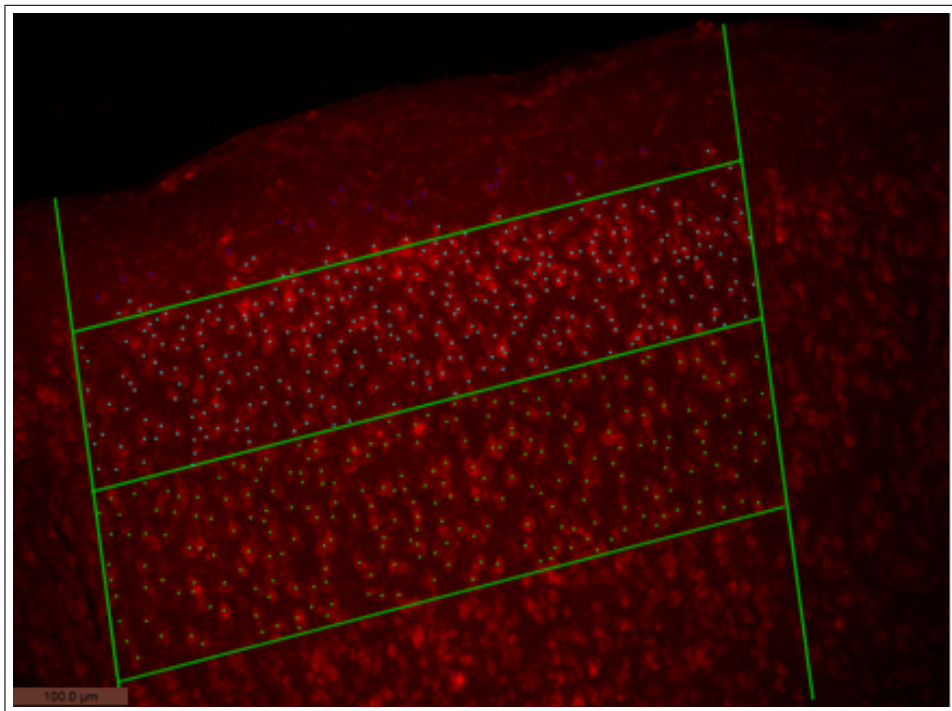


**Figure 4.7** EtBr staining for quantifying the total number of cells in S1HL. Horizontal green lines indicates layer boundaries. Green small dots indicates counted samples (Rat 216-slide 7-Magnification x20).

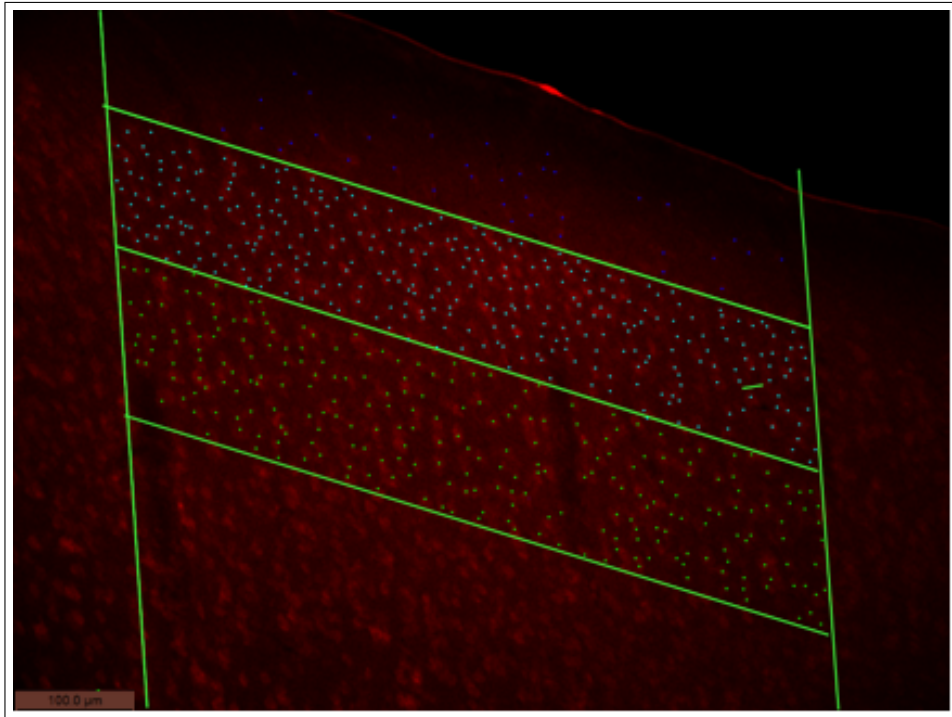


**Figure 4.8** EtBr staining for quantifying the total number of cells in S1HL. Horizontal green lines indicated layer boundaries. Green small dots indicates counted samples (Rat 217-slide 1-Magnification x20).

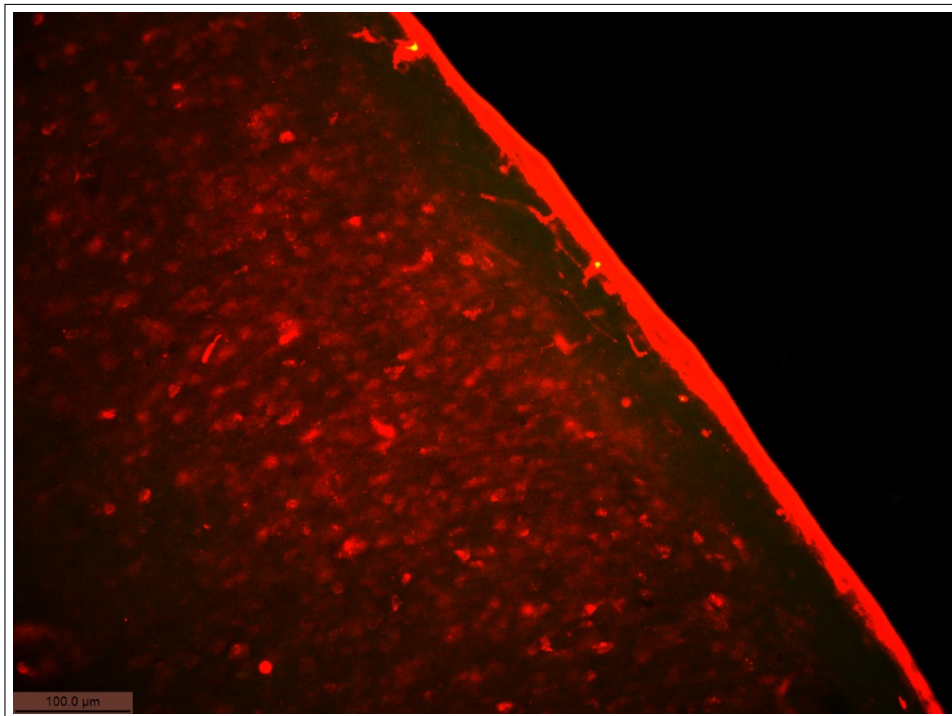


**Figure 4.9** M2 immunostaining in S1BF. (Rat 219-slide 2-Magnification x20).

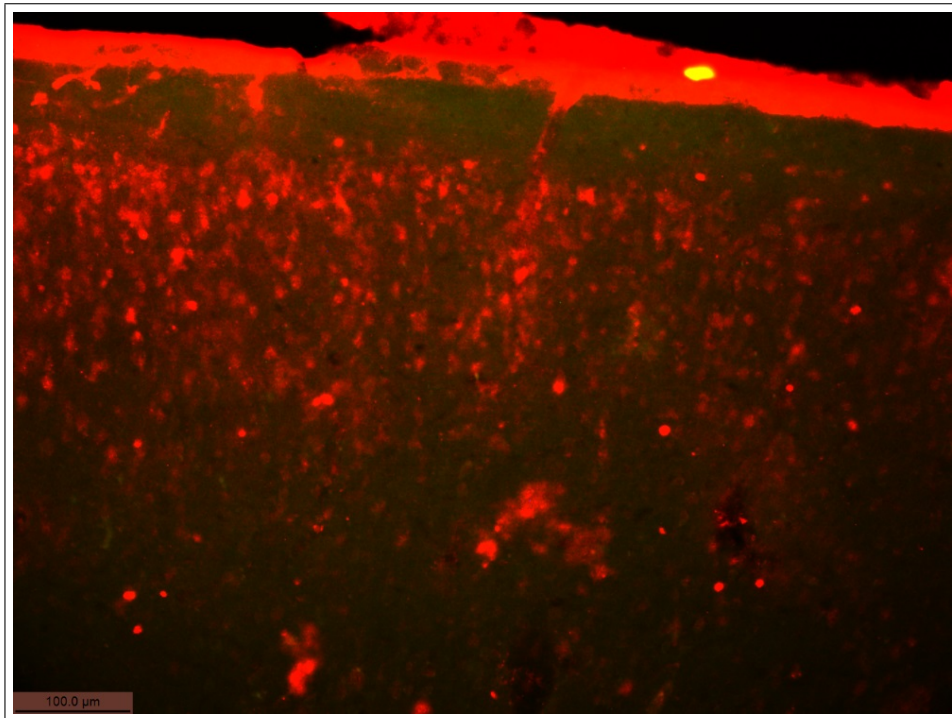


**Figure 4.10** M2 immunostaining in M1. (Rat 222-slide 2-Magnification x20).

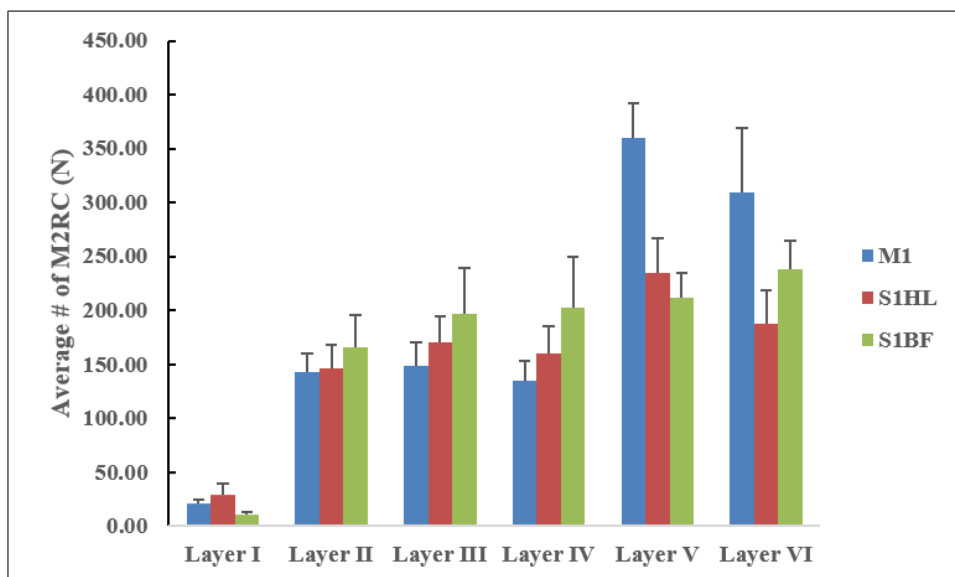


**Figure 4.11** Distribution of average number of M2RC (N) through all layers for each are. All bars are shown as Mean + SEM.

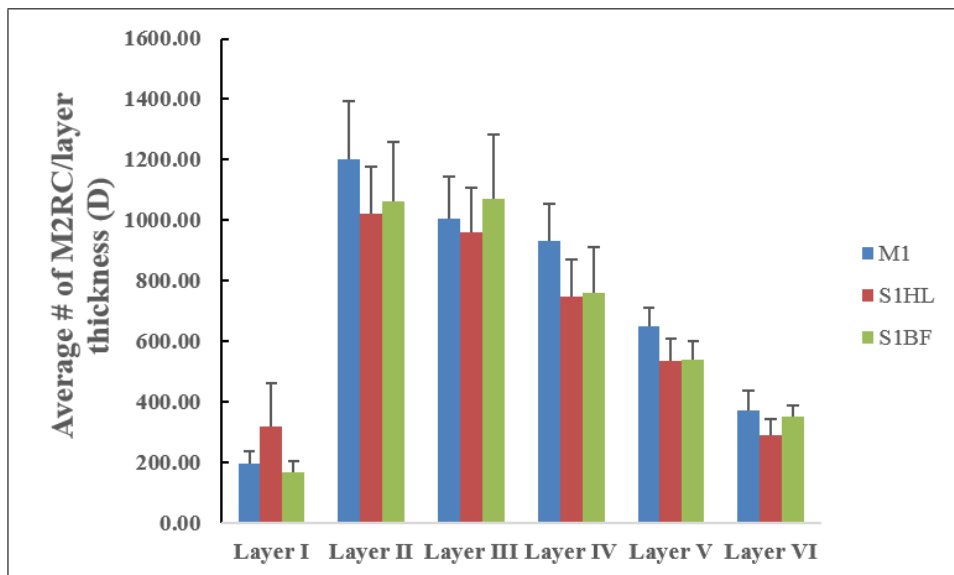


**Figure 4.12** Distribution of average number of M2RC per mm layer thickness (D) through all layers for each area. All bars are shown as Mean + SEM.

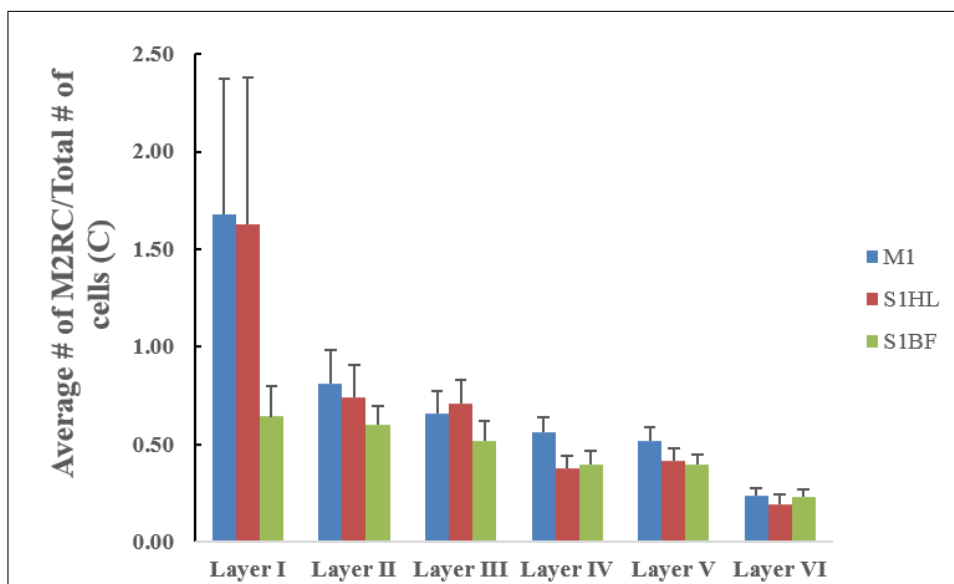


**Figure 4.13** Distribution of average number of M2RC per total number of cells(C) through all layers for each area. All bars are shown as Mean + SEM.

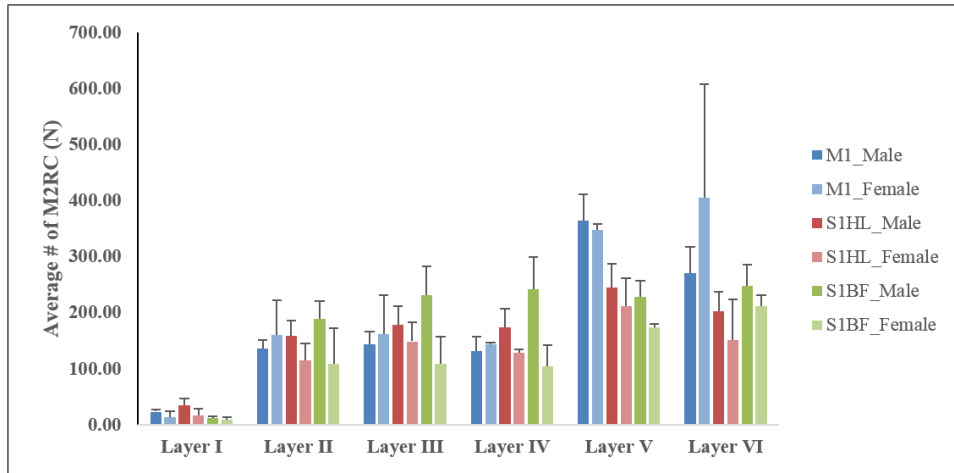


**Figure 4.14** Distribution of average number of M2RC (N) through all layers by sex for each area. All bars are shown as Mean + SEM.

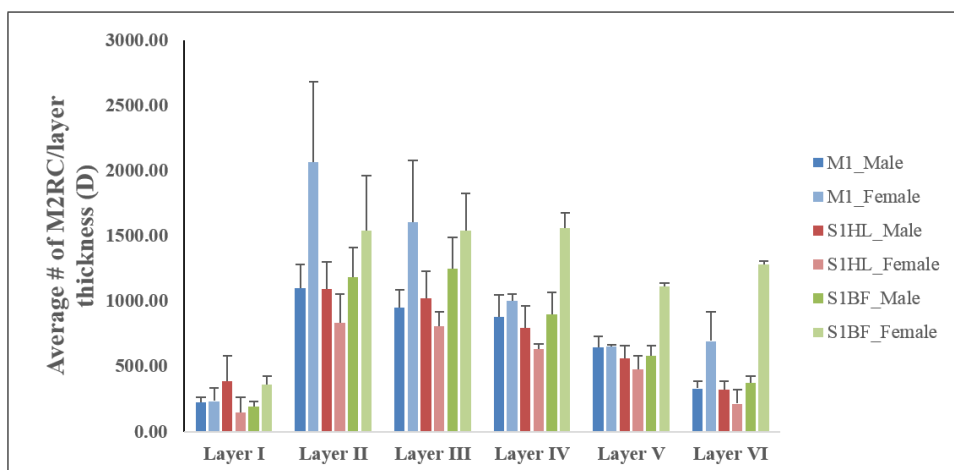


**Figure 4.15** Distribution of average number of M2RC per mm layer thickness (D) through all layers by sex for each area. All bars are shown as Mean + SEM.

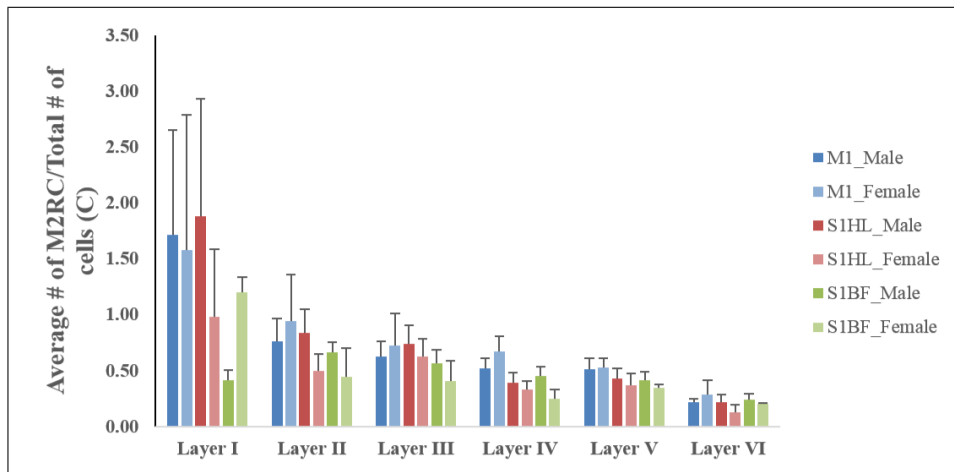


**Figure 4.16** Distribution of average number of M2RC per total number of cells(C) through all layers by sex for each area. All bars are shown as Mean + SEM.

## 5. DISCUSSION and CONCLUSION

The aim of this study was to investigate the detailed cortical layer distribution of the muscarinic receptor M2 and compare the differences between areas in rat: S1HL, S1BF and M1. Previous studies showed the general distribution of cholinergic receptors in parietal cortex and motor cortex. However, the especially the comparison between S1HL and S1BF was not studied. We have successfully showed that although the brain area is not a statistically significant main effect, M2 distribution through the cortical layers is not homogeneous because the projection densities from other brain regions are different. This information will set groundwork for understanding anatomical basis of attentional modulation in the sensorimotor areas of the rat cortex when the distribution of other cholinergic receptors (i.e. specific nicotinic receptors) are investigated. Moreover, our study with Nissl staining revealed cortical differences among three different brain regions.

### 5.1 Comparison of Nissl staining with literature and future work

The Nissl study replicated most of what is known in the literature. There were no differences between the studied areas regarding the thickness of cortical layers I and VI. The nissl staining results which is the control study to compare our calculations for layer thicknesses with the literature showed that there are no differences in layer I and VI with respect to the cortical areas. Layer I and VI receive projections especially from the other layers in the cortex. Additionally, layer VI send feedback projections to thalamus. While extensions of neurons proceed horizontally in layer I, the neurons or their extensions diffuse heterogeneously in layer VI. Layer VI sometimes is considered the transitional layer between grey and white matter [72]. Thus, the cytoarchitecture differences seen here was expected results. As stated in the results, Layer II, III and IV were noticeably thicker than other layers especially in the barrel field. Due to the fact

that signals from the vibrissae pathway is important, which are crucial for navigation and survival, these layer perform complex processing [80]. As expected, the M1 area, also called a granular cortex had a thin layer IV. Some researchers claim that motor cortex does not have layer IV. However, in the protocol of this thesis, layer IV could not be disregarded given the cytoarchitecture observed in the sections. The method used in the experiment may need to be modified in higher resolution to obtain more detailed results. Since layer V is main output layer of cortex, its thickness was especially highest in the M1 area.

Although Nissl staining results were used in present immunohistochemical study for limiting the layers in our thesis, it is also possible to use this information to identify electrode location for neuroprosthetic applications in rat. Movement and feedback can be provided in the prosthesis via electrode arrays placed in S1 and motor cortex. Thus, the locations of the electrodes are significant [81, 82]. The most suitable layer to receive the information from motor cortex is layer V. In order to provide sensory feedback, arrays may be placed on the input layer (layer IV) in the sensory cortex, and with electrical stimulation from layer V and VI, transfer of the information can also be provided as well.

## 5.2 Comparison of immunostaining with previous literature

In the present immunofluorescence study it is clearly demonstrated that high immunoreactivity was seen in all layers except layer I of S1HL, M1 and S1BF for the M2 receptor. The highest number M2RC was found in layer V for M1, and S1HL and in layer VI for S1BF0. As expected higher values were observed in thicker layers. In our study, the highest M2RC density (D) was observed in layers II and III for all three regions. This is consistent with the study conducted by Zee et al. (1992) [7] who showed that muscarinic receptor 2 (M2) were most densely labeled in the layer II, III and IV. Electron and light microscopic investigations of ChAT+ neurons showed that except layer I, almost all cortical layers have consistent ChAT+ neuron bodies [42]. Moreover, the highest density was found both in Layer II and III of M1 and S1. This

verifies that our results are reliable and consistent with ChAT+ staining and former antibody staining results. In the previous studies, M35 antibody was used, but this antibody labeled several muscarinic receptors (i.e. m1-m4 receptor subtypes) [83]. The discrepancies between results can be attributed to methodological differences. In Van der Zee's study [7], sections were taken from the three coronal coordinates (Bregma 1.2, -1.3, -3.3) according to Zilles' Atlas. In the present study, I only studied M2 labeling in serial sections around one coordinate (Bregma -0.4) according to Watson Paxinos Atlas [78]. This may cause some discrepancies. However, my results were similar to those presented in Van der Zee et al [7].

### 5.3 Future work

As explained in detail in the introduction, interactions and contributions of two types cholinergic receptors have a crucial role in higher cognitive processes such as attention, learning and memory [68, 84–87]. It is showed that in Alzheimer's disease(AD), decrease the number of cholinergic neurons in basal forebrain cause presynaptic input depletion to the cerebral cortex. It may reduce the transmission in the cholinceptive neurons which have both nicotinic and muscarinic ACh receptors. Hence, the memory problems occur. The cholinergic hypothesis support the idea that in Alzheimer's disease not only M2 receptors, which are located presynaptically, but also nicotinic  $\alpha 4\beta 2$  receptors decline and the M1 receptors, which are located postsynaptically, protected [88]. It would be important to study distribution of specific nicotinic receptors in the cortex.

In conclusion, this study will also be helpful for setting the groundwork for studying mechanisms underlying the memory impairment e.g. Alzheimer's disease which is directly related the cholinergic system. In addition, the results from the labeling both nicotinic and muscarinic receptors will be utilized to construct the computational model to understand the mechanism and modes of the attention.

## 6. Appendix A

Average number of M2RC for each rat, area, and layer (N). Labeling represents area and layer (e.g. M1-L1 = Motor cortex layer

I)

RAT ID	M1-L1	M1-L2	M1-L3	M1-L4	M1-L5	M1-L6	S1HL-L1	S1HL-L2	S1HL-L3	S1HL-L4	S1HL-L5	S1HL-L6	S1BF-L1	S1BF-L2	S1BF-L3	S1BF-L4	S1BF-L5	S1BF-L6
216	9.95	86.33	59.55	40.71	324.91	235.02	6.32	69.45	62.86	63.41	170.51	271.14	2.96	73.82	58.99	115.51	176.11	214.22
217	3.49	97.37	91.55	139.50	358.03	201.64	3.73	83.87	114.46	122.22	260.90	78.73	3.95	45.29	61.39	66.60	178.99	193.32
218	29.84	147.52	175.26	173.05	524.28	426.24	62.84	223.11	251.08	230.96	414.25	286.43	15.73	251.15	329.73	278.07	299.56	381.95
219	24.04	222.04	231.48	147.09	335.63	607.37	28.20	144.32	182.98	134.56	162.87	222.91	13.86	172.63	157.11	141.30	167.64	230.63
220	22.19	175.01	156.66	106.32	357.16	146.71	16.99	208.54	222.66	206.01	195.15	92.81	11.07	165.22	193.85	95.22	144.99	239.00
221	24.75	116.32	181.97	175.14	378.06	253.15	14.31	136.31	160.92	235.34	231.84	173.00	15.84	243.43	336.13	347.74	249.27	159.45
222	29.65	154.04	146.28	163.23	238.32	294.33	69.58	156.06	195.97	129.80	208.15	189.28	15.04	207.90	240.22	370.50	267.88	245.74
Average	20.56	142.66	148.97	135.00	359.49	309.21	28.85	145.95	170.13	160.33	234.81	187.76	11.21	165.63	196.77	202.14	212.06	237.76
SEM	3.79	17.87	21.79	18.08	32.35	59.64	10.12	21.69	24.31	24.46	32.54	30.49	2.09	30.12	43.06	47.88	22.36	26.53

Average number of M2RC per total number of cells (C) for each rat, area, and layer. Labeling represents area and layer (e.g. M1-L1 = Motor cortex layer I)

RAT ID	M1-L1	M1-L2	M1-L3	M1-L4	M1-L5	M1-L6	S1HL-L1	S1HL-L2	S1HL-L3	S1HL-L4	S1HL-L5	S1HL-L6	S1BF-L1	S1BF-L2	S1BF-L3	S1BF-L4	S1BF-L5	S1BF-L6
216	0.34	0.41	0.27	0.17	0.46	0.23	0.17	0.25	0.23	0.20	0.32	0.47	0.51	0.32	0.13	0.25	0.25	0.23
217	0.38	0.53	0.44	0.81	0.61	0.16	0.37	0.34	0.47	0.41	0.48	0.07	1.06	0.19	0.22	0.17	0.38	0.19
218	0.89	1.29	1.03	0.73	0.90	0.28	2.45	1.53	1.05	0.71	0.79	0.23	0.33	0.78	0.71	0.69	0.68	0.24
219	2.79	1.36	1.01	0.53	0.44	0.42	1.59	0.65	0.78	0.25	0.27	0.19	1.34	0.70	0.59	0.33	0.31	0.21
220	5.35	1.23	0.83	0.60	0.47	0.11	5.75	0.95	1.07	0.49	0.37	0.09	0.71	0.66	0.43	0.25	0.28	0.43
221	1.60	0.31	0.56	0.54	0.41	0.18	0.33	0.57	0.49	0.33	0.32	0.13	0.35	0.82	0.81	0.50	0.36	0.13
222	0.39	0.56	0.45	0.56	0.30	0.28	0.71	0.89	0.86	0.24	0.34	0.16	0.20	0.73	0.73	0.56	0.49	0.20
Average	1.68	0.81	0.66	0.56	0.51	0.24	1.62	0.74	0.71	0.37	0.41	0.19	0.64	0.60	0.52	0.39	0.39	0.23
SEM	0.69	0.17	0.11	0.07	0.07	0.03	0.75	0.16	0.11	0.06	0.06	0.05	0.15	0.09	0.10	0.07	0.05	0.03

Average number of M2RC per layer thickness (D) for each rat, area, and layer. Labeling represents area and layer (e.g. M1-L1 = Motor cortex layer I)

RAT ID	M1-L1	M1-L2	M1-L3	M1-L4	M1-L5	M1-L6	S1HL-L1	S1HL-L2	S1HL-L3	S1HL-L4	S1HL-L5	S1HL-L6	S1BF-L1	S1BF-L2	S1BF-L3	S1BF-L4	S1BF-L5	S1BF-L6
216	91.54	766.72	484.52	343.62	652.09	307.98	55.37	562.43	411.16	349.23	421.24	537.32	358.11	402.79	442.95	561.06	418.11	352.13
217	29.69	839.52	658.64	1107.20	676.69	254.04	33.15	619.78	695.30	671.63	584.60	106.93	49.44	336.90	344.53	307.69	462.90	265.47
218	305.57	1433.90	1268.79	1420.61	967.24	397.69	498.13	1637.08	1310.91	1262.12	954.89	355.20	163.26	1448.27	1705.80	1235.16	782.15	501.56
219	235.80	2065.35	1606.88	1004.77	655.04	695.80	262.00	1052.58	917.15	596.28	368.01	326.11	172.37	1174.65	917.74	536.52	413.69	322.63
220	211.19	1492.99	1105.26	858.77	570.50	172.02	150.35	1131.34	1075.09	1121.78	455.43	141.02	112.90	953.32	929.58	427.01	389.44	451.42
221	275.58	587.19	905.70	847.37	585.33	292.48	143.67	726.04	735.00	710.65	489.05	253.41	169.75	1502.27	1518.47	1017.73	639.88	226.99
222	242.20	1219.67	1001.89	934.35	446.90	494.43	1100.06	1428.99	1573.83	524.10	491.79	319.33	158.15	1616.54	1636.47	1243.62	689.99	354.71
Average	198.80	1200.76	1004.53	930.96	650.54	373.49	320.39	1022.61	959.78	747.97	537.86	291.33	169.14	1062.11	1070.79	761.26	542.31	353.56
SEM	38.05	194.14	141.64	122.81	60.38	66.33	142.74	155.64	149.36	123.77	73.98	54.47	35.65	197.33	212.06	148.89	59.86	36.59

## 7. Appendix B

RAT	LAYER	AREA		
		S1HL	Barrel	M1
183	L1	74.4825	38.48875	70.0075
184	L1	82.659	60.552	73.168
186	L1	95.75275	90.60275	75.39225
191	L1	161.5063	107.5843	169.3047
193	L1	169.3047	169.3047	133.6198
194	L1	51.63467	79.44733	57.87033
195	L1	67.8425	41.688	59.1155
197	L1	64.517	30.59775	61.1385
198	L1	177.4565	77.3085	102.6888
199	L1	156.8035	113.9155	130.0115
183	L2	135.5905	167.4455	113.5788
184	L2	128.9643	168.153	99.11825
186	L2	131.4863	179.6305	107.3715
191	L2	176.7777	177.4013	122.7813
193	L2	205.9845	220.6015	159.3085
194	L2	152.4073	200.5977	150.6683
195	L2	95.2935	125.9335	78.0045
197	L2	93.12225	127.8745	77.45
198	L2	126.3025	135.0035	114.6933
199	L2	133.302	155.1675	117.931
183	L3	161.565	201.2705	144.0288
184	L3	170.1923	197.2523	127.209
186	L3	164.2208	218.0143	123.83
191	L3	216.9933	220.747	152.9053
193	L3	204.293	220.143	186.1453
194	L3	189.8763	221.302	157.1227

*Continued on next page*

*Continued from previous page*

RAT	LAYER	AREA		
		S1HL	Barrel	M1
195	L3	100.3063	143.0415	98.63025
197	L3	128.9123	178.6555	80.66175
198	L3	151.3368	171.2393	127.178
199	L3	172.1975	197.4955	125.5305
183	L4	196.8408	249.3223	159.485
184	L4	237.318	243.8495	143.159
186	L4	166.743	237.6015	129.93
191	L4	209.8923	256.0727	135.7313
193	L4	267.2393	304.6333	147.282
194	L4	203.996	264.4123	138.6513
195	L4	150.5878	207.0488	120.5898
197	L4	206.5923	260.0538	115.9655
198	L4	131.9763	243.9258	111.7818
199	L4	203.5365	201.4585	164.939
184	L5	431.2223	412.2173	472.7713
186	L5	406.381	390.4975	439.221
191	L5	448.8313	391.5897	495.3687
193	L5	441.1683	433.8265	569.8953
194	L5	587.2027	396.0167	829.737
195	L5	380.8943	368.511	406.0118
197	L5	389.495	390.0505	428.5105
198	L5	333.8633	339.8263	355.1868
199	L5	360.999	359.373	392.4555
183	L6	770.433	734.2613	823.3028
184	L6	737.3413	773.5383	851.6183
186	L6	557.3205	739.7368	703.6628
191	L6	528.179	593.8023	666.3577

*Continued on next page*

*Continued from previous page*

		<b>AREA</b>		
<b>RAT</b>	<b>LAYER</b>	<b>S1HL</b>	<b>Barrel</b>	<b>M1</b>
193	L6	568.5858	844.1205	715.9335
194	L6	796.2557	796.729	852.0827
195	L6	482.0275	568.9633	757.3458
197	L6	711.8793	734.0855	734.7765
198	L6	472.4	510.063	531.5333
199	L6	508.635	626.191	670.9695

## REFERENCES

1. Eriksen, C. W., and J. E. Hoffman, "Temporal and spatial characteristics of selective encoding from visual displays," *Perception & Psychophysics*, Vol. 12, no. 2, pp. 201–204, 1972.
2. de Haan, B., P. S. Morgan, and C. Rorden, "Covert orienting of attention and overt eye movements activate identical brain regions," *Brain Research*, Vol. 1204, pp. 102–111, 2008.
3. Perry, E., M. Walker, J. Grace, and R. Perry, "Acetylcholine in mind: a neurotransmitter correlate of consciousness?," *Trends in Neurosciences*, Vol. 22, pp. 273–280, Jun 1999.
4. Sarter, M., and J. P. Bruno, "Abnormal regulation of corticopetal cholinergic neurons and impaired information processing in neuropsychiatric disorders," 1999.
5. Sarter, M., M. E. Hasselmo, J. P. Bruno, and B. Givens, "Unraveling the attentional functions of cortical cholinergic inputs: interactions between signal-driven and cognitive modulation of signal detection.," *Brain Research. Brain Research Reviews*, Vol. 48, pp. 98–111, Feb 2005.
6. Klinkenberg, I., A. Sambeth, and A. Blokland, "Acetylcholine and attention.," *Behavioural Brain Research*, Vol. 221, pp. 430–42, Aug 2011.
7. Zee, A. V. D., C. Streefland, A. D. Strosberg, H. Schröder, and P. G. M. Luiten, "Visualization of cholinergic neurons in the rat neocortex : colocalization of muscarinic and nicotinic acetylcholine receptors," *Molecular Brain Research*, Vol. 14, pp. 326–336, 1992.
8. Luiten, P. G., G. I. de Jong, E. a. Van der Zee, and H. van Dijken, "Ultrastructural localization of cholinergic muscarinic receptors in rat brain cortical capillaries.," *Brain Research*, Vol. 720, no. 1-2, pp. 225–229, 1996.
9. Okuda, H., S. Shioda, Y. Nakai, H. Nakayama, M. Okamoto, and T. Nakashima, "Immunocytochemical localization of nicotinic acetylcholine receptor in rat hypothalamus," *Brain Research*, Vol. 625, no. 1, pp. 145–151, 1993.
10. van der Zee, E. A., C. Streefland, A. D. Strosberg, H. Schröder, and P. G. Luiten, "Colocalization of muscarinic and nicotinic receptors in cholinergic neurons of the suprachiasmatic region in young and aged rats," *Brain Research*, Vol. 542, no. 2, pp. 348–352, 1991.
11. van der Zee, E. A., A. D. Strosberg, B. Bohus, and P. G. M. Luiten, "Colocalization of muscarinic acetylcholine receptors and protein kinase C  $\gamma$  in rat parietal cortex," *Molecular Brain Research*, Vol. 18, no. 1-2, pp. 152–162, 1993.
12. Zilles, K., H. Schröder, U. Schröder, E. Horvath, L. Werner, P. G. M. Luiten, A. Maelicke, and A. D. Strosberg, "Distribution of cholinergic receptors in the rat and human neocortex," in *Central Cholinergic Synaptic Transmission*, pp. 212–228, Birkhäuser Basel, 1989.
13. VandenBos, G. R., *APA dictionary of psychology*, American Psychological Association, 2007.

14. Bartus, R. T., R. L. Dean, B. Beer, and A. S. Lippa, "The cholinergic hypothesis of geriatric memory dysfunction.," *Science (New York, N.Y.)*, Vol. 217, pp. 408–14, Jul 1982.
15. Bartus, R. T., R. L. Dean, M. J. Pontecorvo, and C. Flicker, "The cholinergic hypothesis: a historical overview, current perspective, and future directions.," *Annals of the New York Academy of Sciences*, Vol. 444, pp. 332–58, 1985.
16. Bentley, P., P. Vuilleumier, C. M. Thiel, J. Driver, and R. J. Dolan, "Cholinergic enhancement modulates neural correlates of selective attention and emotional processing.," *NeuroImage*, Vol. 20, pp. 58–70, Sep 2003.
17. Purves, D., G. J. Augustine, D. Fitzpatrick, W. C. Hall, A.-S. Lamantia, J. O. Mcnamara, and S. M. Willians, *Neuroscience*, Vol. 3, 2004.
18. Theeuwes, J., "Exogenous and endogenous control of attention: the effect of visual onsets and offsets.," *Perception & Psychophysics*, Vol. 49, pp. 83–90, Jan 1991.
19. Posner, M. I., and S. E. Petersen, "The attention system of the human brain.," *Annual Review of Neuroscience*, Vol. 13, pp. 25–42, 1990.
20. Hodgson, T. L., and H. J. Müller, "Attentional Orienting in Two-dimensional Space," *The Quarterly Journal of Experimental Psychology Section A*, Vol. 52, pp. 615–648, Aug 1999.
21. Posner, M. I., and M. K. Rothbart, "Attention, self-regulation and consciousness.," *Philosophical Transactions of The Royal Society of London. Series B, Biological Sciences*, Vol. 353, pp. 1915–27, Nov 1998.
22. Himmelheber, A. M., M. Sarter, and J. P. Bruno, "The effects of manipulations of attentional demand on cortical acetylcholine release," *Cognitive Brain Research*, Vol. 12, pp. 353–370, Dec 2001.
23. Fernández de Sevilla, D., C. Cabezas, A. N. O. de Prada, A. Sánchez-Jiménez, and W. Buño, "Selective muscarinic regulation of functional glutamatergic Schaffer collateral synapses in rat CA1 pyramidal neurons.," *The Journal of Physiology*, Vol. 545, pp. 51–63, Nov 2002.
24. Linster, C., M. Maloney, M. Patil, and M. E. Hasselmo, "Enhanced cholinergic suppression of previously strengthened synapses enables the formation of self-organized representations in olfactory cortex.," *Neurobiology of Learning and Memory*, Vol. 80, pp. 302–14, Nov 2003.
25. Acquas, E., C. Wilson, and H. C. Fibiger, "Conditioned and unconditioned stimuli increase frontal cortical and hippocampal acetylcholine release: effects of novelty, habituation, and fear.," *The Journal of Neuroscience : The Official Journal of The Society for Neuroscience*, Vol. 16, pp. 3089–96, May 1996.
26. Turchi, J., and M. Sarter, "Cortical acetylcholine and processing capacity: Effects of cortical cholinergic deafferentation on crossmodal divided attention in rats," *Cognitive Brain Research*, Vol. 6, no. 2, pp. 147–158, 1997.
27. Arnold, H. M., J. A. Burk, E. M. Hodgson, M. Sarter, and J. P. Bruno, "Differential cortical acetylcholine release in rats performing a sustained attention task versus behavioral control tasks that do not explicitly tax attention," *Neuroscience*, Vol. 114, no. 2, pp. 451–460, 2002.

28. Himmelheber, A. M., M. Sarter, and J. P. Bruno, "Increases in cortical acetylcholine release during sustained attention performance in rats.," *Brain Research. Cognitive Brain Research*, Vol. 9, no. 3, pp. 313–325, 2000.
29. McGaughy, J., and M. Sarter, "Sustained attention performance in rats with intracortical infusions of 192 IgG-saporin-induced cortical cholinergic deafferentation: effects of physostigmine and FG 7142.," *Behavioral Neuroscience*, Vol. 112, no. 6, pp. 1519–1525, 1998.
30. Oldford, E., and M. A. Castro-Alamancos, "Input-specific effects of acetylcholine on sensory and intracortical evoked responses in the "barrel cortex" in vivo," *Neuroscience*, Vol. 117, no. 3, pp. 769–778, 2003.
31. Fournier, G. N., K. Semba, and D. D. Rasmusson, "Modality- and region-specific acetylcholine release in the rat neocortex.," *Neuroscience*, Vol. 126, pp. 257–62, Jan 2004.
32. Inglis, F. M., and H. C. Fibiger, "Increases in hippocampal and frontal cortical acetylcholine release associated with presentation of sensory stimuli.," *Neuroscience*, Vol. 66, pp. 81–6, May 1995.
33. Paterson, D., and A. Nordberg, "Neuronal nicotinic receptors in the human brain.," *Progress in Neurobiology*, Vol. 61, pp. 75–111, May 2000.
34. Bloem, B., R. B. Poorthuis, and H. D. Mansvelder, "Cholinergic modulation of the medial prefrontal cortex: the role of nicotinic receptors in attention and regulation of neuronal activity.," *Frontiers in Neural Circuits*, Vol. 8, p. 17, 2014.
35. Corringer, P.-J., N. L. Novère, and J.-P. Changeux, "Nicotinic Receptors at the Amino Acid Level," *Annual Review of Pharmacology and Toxicology*, Vol. 40, pp. 431–458, Apr 2000.
36. Lukas, R. J., J. P. Changeux, N. Le Novère, E. X. Albuquerque, D. J. Balfour, D. K. Berg, D. Bertrand, V. A. Chiappinelli, P. B. Clarke, A. C. Collins, J. A. Dani, S. R. Grady, K. J. Kellar, J. M. Lindstrom, M. J. Marks, M. Quik, P. W. Taylor, and S. Wonnacott, "International Union of Pharmacology. XX. Current status of the nomenclature for nicotinic acetylcholine receptors and their subunits.," *Pharmacological Reviews*, Vol. 51, pp. 397–401, Jun 1999.
37. Gotti, C., and F. Clementi, "Neuronal nicotinic receptors: from structure to pathology," *Progress in Neurobiology*, Vol. 74, pp. 363–396, Dec 2004.
38. Zoli, M., C. Lena, M. R. Picciotto, and J.-P. Changeux, "Identification of Four Classes of Brain Nicotinic Receptors Using B2 Mutant Mice," *The Journal of Neuroscience*, Vol. 18, no. 12, pp. 4461–4472, 1998.
39. Sharples, C. G. V., and S. Wonnacott, "Neuronal nicotinic receptors," *Tocris Reviews*, Vol. 19, pp. 1–12, 2001.
40. Hendrickson, L. M., M. J. Guildford, and A. R. Tapper, "Neuronal Nicotinic Acetylcholine Receptors: Common Molecular Substrates of Nicotine and Alcohol Dependence," *Frontiers in Psychiatry*, Vol. 4, p. 29, 2013.

41. Clarke, P. B., R. D. Schwartz, S. M. Paul, C. B. Pert, and A. Pert, "Nicotinic binding in rat brain: autoradiographic comparison of [3H]acetylcholine, [3H]nicotine, and [125I]-alpha-bungarotoxin.," *The Journal of Neuroscience : The Official Journal of The Society for Neuroscience*, Vol. 5, pp. 1307–15, May 1985.
42. Houser, C. R., G. D. Crawford, P. M. Salvaterra, and J. E. Vaughn, "Immunocytochemical localization of choline acetyltransferase in rat cerebral cortex: a study of cholinergic neurons and synapses.," *The Journal of Comparative Neurology*, Vol. 234, pp. 17–34, Apr 1985.
43. Tribollet, E., D. Bertrand, A. Marguerat, and M. Raggenbass, "Comparative distribution of nicotinic receptor subtypes during development, adulthood and aging: an autoradiographic study in the rat brain.," *Neuroscience*, Vol. 124, pp. 405–420, Jan 2004.
44. Clarke, P. B., C. B. Pert, and A. Pert, "Autoradiographic distribution of nicotine receptors in rat brain.," *Brain Research*, Vol. 323, pp. 390–5, Dec 1984.
45. Sahin, M., W. D. Bowen, and J. P. Donoghue, "Location of nicotinic and muscarinic cholinergic and u-opiate receptors in rat cerebral neocortex: Evidence from thalamic and cortical lesions," *Brain Research*, Vol. 579, pp. 135–147, 1992.
46. Clarke, P. B., "Nicotinic modulation of thalamocortical neurotransmission," *Progress in Brain Research*, Vol. 145, pp. 253–260, 2004.
47. London, E. D., S. B. Waller, and J. K. Wamsley, "Autoradiographic localization of [3H]nicotine binding sites in the rat brain," *Neuroscience Letters*, Vol. 53, pp. 179–184, Jan 1985.
48. Metherate, R., "Nicotinic acetylcholine receptors in sensory cortex.," *Learning & Memory*, Vol. 11, no. 1, pp. 50–9, 2004.
49. Levy, R. B., A. D. Reyes, and C. Aoki, "Nicotinic and muscarinic reduction of unitary excitatory postsynaptic potentials in sensory cortex; dual intracellular recording in vitro.," *Journal of Neurophysiology*, Vol. 95, pp. 2155–66, Apr 2006.
50. Christophe, E., A. Roebuck, J. F. Staiger, D. J. Lavery, E. Audinat, A. J. Lee, G. Wang, X. Jiang, S. M. Johnson, E. T. Hoang, R. L. Stornetta, M. P. Beenhakker, Y. Shen, J. J. Zhu, A. Brombas, L. N. Fletcher, and S. R. Williams, "Two Types of Nicotinic Receptors Mediate an Excitation of Neocortical Layer I Interneurons," *Journal of Neurophysiology*, Vol. 88, pp. 1318–1327, 2002.
51. Xiang, Z., J. R. Huguenard, and D. A. Prince, "Cholinergic switching within neocortical inhibitory networks.," *Science (New York, N.Y.)*, Vol. 281, pp. 985–988, 1998.
52. Nuñez, A., S. Domínguez, W. Buño, and D. Fernández de Sevilla, "Cholinergic-mediated response enhancement in barrel cortex layer V pyramidal neurons.," *Journal of Neurophysiology*, Vol. 108, pp. 1656–68, Sep 2012.
53. Albuquerque, E. X., E. F. R. Pereira, M. Alkondon, and S. W. Rogers, "Mammalian Nicotinic Acetylcholine Receptors: From Structure to Function," *Physiology Review*, Vol. 89, no. 1, pp. 73–120, 2009.
54. Chen, D., and J. W. Patrick, "The alpha-bungarotoxin-binding nicotinic acetylcholine receptor from rat brain contains only the alpha7 subunit.," *The Journal of Biological Chemistry*, Vol. 272, pp. 24024–9, Sep 1997.

55. Sillito, A. M., and P. C. Murphy, "The Cholinergic Modulation of Cortical Function," pp. 161–185, Springer, Boston, MA, 1987.
56. Caulfield, M. P., and N. J. Birdsall, "International Union of Pharmacology. XVII. Classification of muscarinic acetylcholine receptors.," *Pharmacological Reviews*, Vol. 50, pp. 279–90, Jun 1998.
57. Bonner, T. I., N. J. Buckley, A. C. Young, and M. R. Brann, "Identification of a family of muscarinic acetylcholine receptor genes," *Science*, Vol. 237, pp. 527–532, 1987.
58. Levey, A. I., C. A. Kitt, W. F. Simonds, D. L. Price, and M. R. Brann, "Identification and localization of muscarinic acetylcholine receptor proteins in brain with subtype-specific antibodies.," *The Journal of Neuroscience : The Official Journal of The Society for Neuroscience*, Vol. 11, pp. 3218–3226, 1991.
59. Levin, E. D., J. E. Rose, S. R. McGurk, and L. L. Butcher, "Characterization of the cognitive effects of combined muscarinic and nicotinic blockade.," *Behavioral and Neural Biology*, Vol. 53, pp. 103–112, 1990.
60. Erisir, A., A. I. Levey, and C. Aoki, "Muscarinic receptor M(2) in cat visual cortex: laminar distribution, relationship to gamma-aminobutyric acidergic neurons, and effect of cingulate lesions.," *The Journal of Comparative Neurology*, Vol. 441, pp. 168–85, Dec 2001.
61. Mrzljak, L., A. I. Levey, and P. S. Goldman-Rakic, "Association of m1 and m2 muscarinic receptor proteins with asymmetric synapses in the primate cerebral cortex: morphological evidence for cholinergic modulation of excitatory neurotransmission.," *Proceedings of the National Academy of Sciences of the United States of America*, Vol. 90, pp. 5194–8, Jun 1993.
62. Walch, L., C. Brink, and X. Norel, "The muscarinic receptor subtypes in human blood vessels," 2001.
63. Potter, L. T., D. D. Flynn, J.-S. Liang, and M. H. McCollum, "Studies of muscarinic neurotransmission with antimuscarinic toxins," in *Progress in brain research*, Vol. 145, pp. 121–128, 2004.
64. Hasselmo, M. E., and M. Cekić, "Suppression of synaptic transmission may allow combination of associative feedback and self-organizing feedforward connections in the neocortex.," *Behavioural Brain Research*, Vol. 79, pp. 153–61, Sep 1996.
65. Gil, Z., B. W. Connors, and Y. Amitai, "Differential regulation of neocortical synapses by neuromodulators and activity.," *Neuron*, Vol. 19, pp. 679–86, Sep 1997.
66. McKenna, T. M., J. H. Ashe, G. K. Hui, and N. M. Weinberger, "Muscarinic agonists modulate spontaneous and evoked unit discharge in auditory cortex of cat," *Synapse*, Vol. 2, no. 1, pp. 54–68, 1988.
67. Metherrate, R., N. Tremblay, and R. W. Dykes, "The Effects of Acetylcholine on Response Properties of Cat Somatosensory Cortical Neurons," *Journal of Neurophysiology*, Vol. 59, no. 4, pp. 1231–1252, 1988.
68. Levin, E. D., S. R. McGurk, D. South, and L. L. Butcher, "Effects of combined muscarinic and nicotinic blockade on choice accuracy in the radial-arm maze.," *Behavioral and Neural Biology*, Vol. 51, pp. 270–277, 1989.

69. Tanahashi, Y., T. Unno, H. Matsuyama, T. Ishii, M. Yamada, J. Wess, and S. Komori, "Multiple muscarinic pathways mediate the suppression of voltage-gated  $Ca^{2+}$  channels in mouse intestinal smooth muscle cells," *British Journal of Pharmacology*, Vol. 158, no. 8, pp. 1874–1883, 2009.
70. Gerhard, D., "Biological Psychology: An Introduction to Behavioral, Cognitive, and Clinical Neuroscience," *The Yale Journal of Biology and Medicine*, Vol. 86, no. 3, p. 435, 2013.
71. Herculano-Houzel, S., "The human brain in numbers: a linearly scaled-up primate brain," *Frontiers in Human Neuroscience*, Vol. 3, p. 31, Nov 2009.
72. Kandel, E. R., *Principles of Neural Science, Fifth Edition*, 2013.
73. Young, B. P., G. O'Dowd, and P. Woodford, *Wheater's functional histology : a text and colour atlas*.
74. Kristt, D. A., "Somatosensory cortex: acetylcholinesterase staining of barrel neuropil in the rat.," *Neuroscience Letters*, Vol. 12, pp. 177–82, May 1979.
75. Houser, C. R., G. D. Crawford, R. P. Barber, P. M. Salvaterra, and J. E. Vaughn, "Organization and morphological characteristics of cholinergic neurons: an immunocytochemical study with a monoclonal antibody to choline acetyltransferase.," *Brain Research*, Vol. 266, pp. 97–119, Apr 1983.
76. "Gel Imaging | How to Select LED Color."
77. "<https://jireurope.com/technical/products/conjugate-selection/alexa-fluor/594>,"
78. Paxinos, G., and C. Watson, *The Rat Brain in Stereotaxic Coordinates*, Academic Press, 3 ed., 1997.
79. Schneider, C. A., W. S. Rasband, and K. W. Eliceiri, "NIH Image to ImageJ: 25 years of image analysis," *Nature Methods*, Vol. 9, pp. 671–675, Jul 2012.
80. Ahissar, E., "And motion changes it all," *Nature Neuroscience*, Vol. 11, no. 12, pp. 1369–1370, 2008.
81. Shanechi, M. M., R. C. Hu, and Z. M. Williams, "A cortical-spinal prosthesis for targeted limb movement in paralysed primate avatars.," *Nature Communications*, Vol. 5, p. 3237, 2014.
82. Tabot, G. a., J. F. Dammann, J. a. Berg, F. V. Tenore, J. L. Boback, R. J. Vogelstein, and S. J. Bensmaia, "Restoring the sense of touch with a prosthetic hand through a brain interface.," *Proceedings of the National Academy of Sciences of the United States of America*, Vol. 110, no. 45, pp. 18279–84, 2013.
83. Carsi-Gabrenas, J. M., E. A. Van Der Zee, P. G. M. Luiten, and L. T. Potter, "Non-selectivity of the monoclonal antibody M35 for subtypes of muscarinic acetylcholine receptors," *Brain Research Bulletin*, Vol. 44, no. 1, pp. 25–31, 1997.
84. Levin, E. D., F. J. McClernon, and A. H. Rezvani, "Nicotinic effects on cognitive function: behavioral characterization, pharmacological specification, and anatomic localization.," *Psychopharmacology*, Vol. 184, pp. 523–39, Mar 2006.

85. Levin, E. D., and J. E. Rose, "Nicotinic and muscarinic interactions and choice accuracy in the radial-arm maze.," *Brain Research Bulletin*, Vol. 27, pp. 125–8, Jul 1991.
86. Riekkinen, P., J. Sirviö, M. Aaltonen, and P. Riekkinen, "Effects of concurrent manipulations of nicotinic and muscarinic receptors on spatial and passive avoidance learning.," *Pharmacology, Biochemistry, and Behavior*, Vol. 37, pp. 405–10, nov 1990.
87. Tilson, H. A., R. L. McLamb, S. Shaw, B. C. Rogers, P. Pediaditakis, and L. Cook, "Radial-arm maze deficits produced by colchicine administered into the area of the nucleus basalis are ameliorated by cholinergic agents.," *Brain Research*, Vol. 438, pp. 83–94, Jan 1988.
88. Eglen, R. M., "Overview of Muscarinic Receptor Subtypes," in *Handbook of experimental pharmacology*, no. 208, pp. 3–28, 2012.